ORGANOMETALLICS

pubs.acs.org/Organometallics Article

Cycloneophylpalladium(IV) Complexes: Formation by Oxidative Addition and Selectivity of Their Reductive Elimination Reactions

Ava Behnia, Mahmood A. Fard, Johanna M. Blacquiere,* and Richard J. Puddephatt*

Cite This: https://dx.doi.org/10.1021/acs.organomet.0c00615 Read Online

ACCESS | Metrics & More | Article Recommendations | Supporting Information

ABSTRACT: The cycloneophylpalladium(II) complexes [Pd($CH_2CMe_2C_6H_4$)(κ^2-*N*,*N*′-**L**)] (**L** = $RO(CH_2)_3N(CH_2{-}2{-}C_5H_4N)_2$, R = H, Me) undergo oxidation to Pd(IV) with bromine or iodine to give [PdX($CH_2CMe_2C_6H_4$)(κ^3-*N*,*N*′,*N*″-**L**)]X (X = Br, I) or with methyl iodide to give the transient complexes [PdMe($CH_2CMe_2C_6H_4$)(κ^3-*N*,*N*′,*N*″-**L**)]I. The products of Br_2 and I_2 oxidation, [PdX($CH_2CMe_2C_6H_4$)(κ^3-*N*,*N*′,*N*″-**L**)]X (X = Br, I), are sufficiently stable to be isolated, but they decompose slowly in solution by reductive elimination to give the palladium(II) products [PdX(κ^3-*N*,*N*′,*N*″-**L**)]X (X = Br, I). The organic products are formed via either CH_2−Ar or CH_2−X bond formation. In the latter case, neophyl rearrangement and protonolysis steps follow reductive elimination to give a mixture of organic products. The methylpalladium(IV) complexes [PdMe($CH_2CMe_2C_6H_4$)(κ^3-*N*,*N*′,*N*″-**L**)]I decompose at 0 °C by selective reductive elimination with Me−Ar bond coupling to give the alkylpalladium(II) complex [Pd(CH_2CMe_2-2-C_6H_4Me)(κ^3-*N*,*N*′,*N*″-**L**)]I. The mechanisms of the reactions have been explored by kinetic studies.

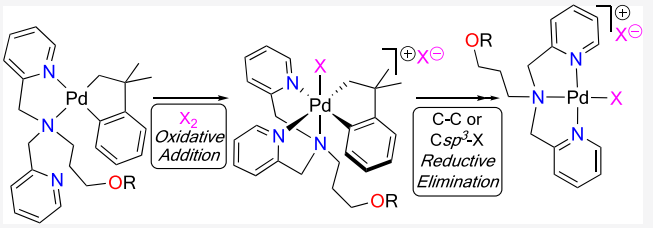

INTRODUCTION

It is now well established that Pd(II)/Pd(IV) cycles are important in catalysis by palladium complexes, especially in reactions involving strong oxidants such as halogens, dioxygen, and peroxides.[1,2] For example, the catalytic reaction of iodine with alkanes or arenes to form iodo-containing hydrocarbons is thought to involve alkane C−H bond activation to form an alkylpalladium(II) complex, followed by oxidative addition of iodine and then reductive elimination from palladium(IV).[3−5] These impressive advances have stimulated further efforts to understand the factors that affect reactivity and selectivity in oxidative addition at palladium(II) and reductive elimination from palladium(IV) complexes.[6−18] In studies of selectivity in reductive elimination, the cycloneophylpalladium(IV) complexes have played an important role as a model to distinguish between reactivity at C(sp^2) or C(sp^3) centers.[2,8,13,14,18−29] When the palladium(IV) complexes (***A***) are sufficiently stable to be isolated, the mechanisms of reductive elimination have been studied and, in most cases, have been shown to involve five-coordinate intermediates such as ***B*** (Scheme 1).[19−22,24] External nucleophilic attack on such intermediates occurs selectively at the CH_2 group and can lead, for example, to C−O or C−N bond formation (Scheme 1a). If the supporting ligand can access a facial tridentate coordination mode, as in ***D***, intramolecular X−Ar reductive elimination from the six-coordinate complex is proposed to give ***F*** (Scheme 1b).[25]

With cycloneophylpalladium complexes, there have been few studies of oxidative addition−reductive elimination by reaction with bromine, iodine, or methyl iodide.[25,28] The complex ***D***, where X = I, formed by oxidative addition of iodine to the Pd(II) precursor, but this derivative is stable to reductive elimination.[25] On the other hand, the diimine complex

Scheme 1. Reductive Elimination from Pd(IV) with (a) CH_2−X Bond Formation (X = OR, NR_2) or (b) Ar−X Bond Formation (X = OH, L = Solvent dmso)

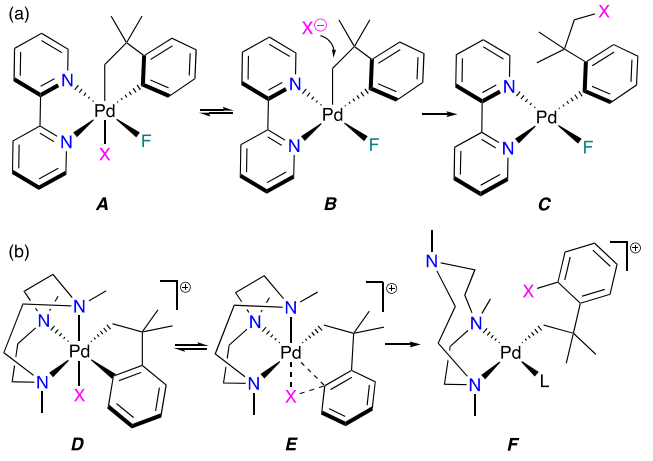

Received: September 16, 2020

[Pd(CH$_2$CMe$_2$C$_6$H$_4$)(MesN═CHCH═NMes)] (***G***) reacts with bromine or iodine to give the palladium(II) dihalide complex ***I*** and the cyclobutane derivative **CB**, probably by way of a palladium(IV) intermediate ***H*** that could not be detected (Scheme 2).[28] With hydrogen peroxide ***G*** gives the oxygen

Scheme 2. Reductive Coupling from Proposed Five-Coordinate Intermediates *H*, by either C−C Reductive Elimination to Give Cyclobutane Derivative CB or by Oxygen-Atom Insertion to Give *J*

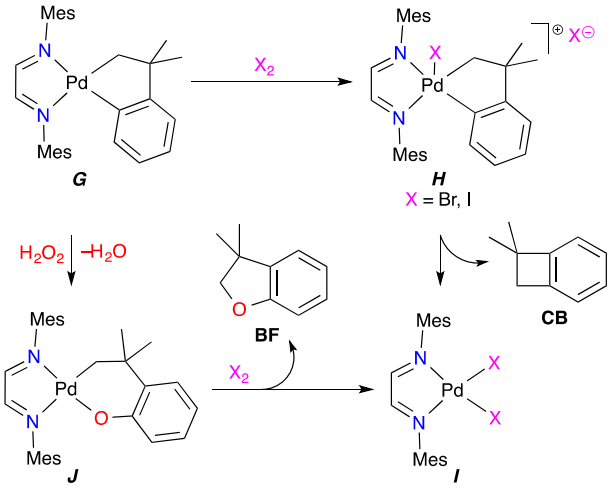

atom insertion product ***J***. Further reaction with bromine or iodine gave the benzofuran derivative **BF** and the palladium(II) complexes ***I***, but again no palladium(IV) intermediate could be detected. The present article reports related chemistry in which palladium(IV) intermediates can be isolated, or at least detected, but which also undergo facile reductive elimination to give either C−C or C−X bond formation. This allows a detailed study of the mechanism and selectivity of the reductive elimination steps.

RESULTS AND DISCUSSION

Synthesis of Cycloneophylpalladium(II) Complexes. The cycloneophylpalladium(II) complexes (**1** and **2**) used in this work include the ligands RO(CH$_2$)$_3$N(CH$_2$-2-C$_5$H$_4$N)$_2$ (R = H (**L1**), Me (**L2**)), which coordinate to the metal in a bidentate mode via the tertiary amine and one pyridyl group (Scheme 3).[29−31] The second pyridyl group of **L1** and **L2** gives these ligands the potential to be tridentate, which should stabilize the palladium(IV) oxidation state. They also carry a 3-hydroxypropyl (**L1**) or 3-methoxypropyl substituent (**L2**), with the possibility that **L1** might take part in hydrogen-bonding interactions.[29] The complex [Pd(CH$_2$CMe$_2$C$_6$H$_4$)(κ^2-*N*,*N*′-**L1**)] (**1**) was reported previously, and it was shown to be fluxional (Scheme 3).[29] The ligand binds through the central amine donor and one of the 2-pyridyl groups and might exist primarily as either isomer **1a** or **1b**, which interconvert rapidly through the proposed five-coordinate intermediate **1***. The new complex **2** behaves similarly, as shown by the variable-temperature ^{1}H NMR spectra (Figure 1). At room temperature the two pyridylmethyl groups of coordinated **L2** gave rise to a single broad resonance at δ 8.49 for the pyridyl protons H6a and H6b and another broad resonance at δ 4.13 for the methylene protons H7a and H7b. Each of these broad signals split at −30 °C, to give separate resonances for H6b and H6a

Scheme 3. Synthesis of Complexes 1[29] and 2, Which Are Observed as a Fluxional Mixture Assigned as 1a or 2a and 1b or 2b That Likely Interconvert via 1* or 2*, Respectively[a]

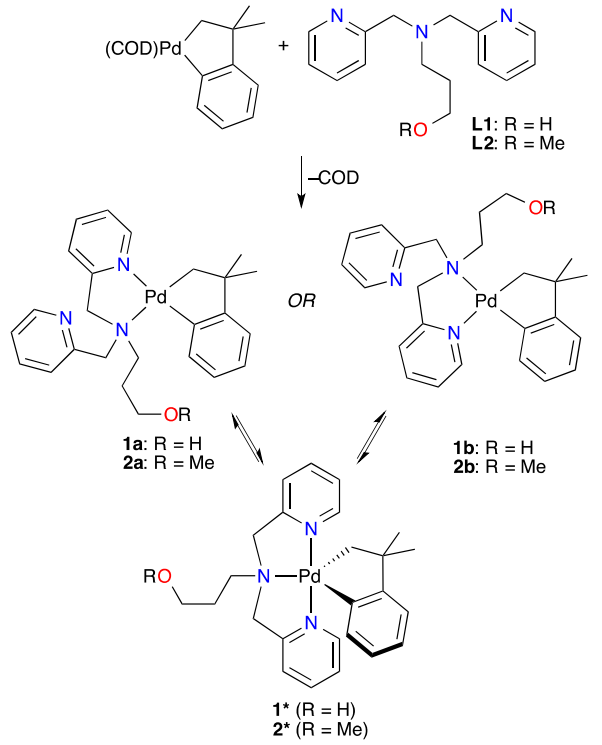

[a]Isolated yield of **2** 75%.

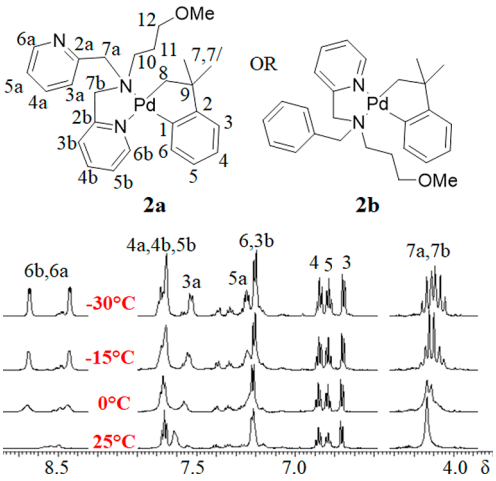

Figure 1. Diagnostic regions of the ^{1}H NMR spectra (600 MHz, CD_2Cl_2 solution) of complex **2** at different temperatures.

(δ 8.63 and 8.43) and to give four overlapping resonances for the nonequivalent methylene protons (δ 4.06−4.17). A ^{1}H−^{1}H NOESY experiment at −30 °C did not give any correlations between the hydrocarbon ligand and **L2**; thus, it is uncertain if the major isomer is **2a** or **2b**. The complexes will be referred to as **1** and **2** in the discussion below, but the isomeric structure shown will be arbitrary.

Oxidation with Bromine and Iodine to Give Palladium(IV) Complexes. The complexes **1** and **2** reacted rapidly with iodine or bromine in chloroform at room temperature to give the corresponding cationic palladium(IV)

https://dx.doi.org/10.1021/acs.organomet.0c00615
Organometallics XXXX, XXX, XXX−XXX

complexes [PdX($CH_2CMe_2C_6H_4$)(κ^3-*N*,*N*′,*N*″-**L**)][X] (**3** (X = I, **L** = **L1**), **4** (X = I, **L** = **L2**), **5** (X = Br, **L** = **L1**), and **6** (X = Br, **L** = **L2**); Scheme 4). The complexes have no symmetry,

Scheme 4. Oxidative Addition Reaction of Complexes 1 and 2 with Iodine and Bromine to Give Complexes 3−6 and Slower Reductive Elimination to Give Complexes 7−10[a]

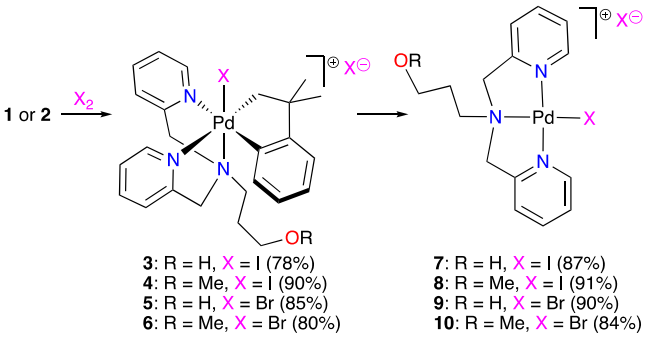

[a]Isolated yields given in parentheses.

and many isomers are possible, but they were formed as single stereoisomers, as indicated by their ^{1}H NMR spectra. These palladium(IV) complexes **3**−**6** were isolated (78−90% yield) in pure form and could be stored at −5 °C as solid samples for several weeks without noticeable decomposition. However, they decomposed slowly in solution at room temperature and more rapidly at 50 °C, to give the corresponding palladium(II) complexes **7**−**10** (84−91% yield), with loss of the cycloneophyl group (Scheme 4). The cationic complex **4** was also prepared as the tetrafluoroborate salt [PdI($CH_2CMe_2C_6H_4$)(κ^3-*N*,*N*′,*N*″-**L2**)][BF_4] (**4a**) in 80% yield by the reaction of complex **2** with the oxidant bis(pyridine)iodonium tetrafluoroborate. Complex **4a** was significantly more stable than the corresponding iodide salt, **4**.

The palladium(IV) complexes **3**−**6** were fully characterized by ^{1}H and ^{13}C NMR spectroscopy, including correlated ^{1}H−^{1}H COSY, ^{1}H−^{1}H NOESY, and ^{1}H−^{13}C HSQC and HMBC NMR spectroscopy, as well as by ESI mass spectrometry and IR spectroscopy. Complex **3**, for example, showed a peak due to ν(OH) of **L1** centered at 3103 cm^{-1} in the IR spectrum. The ^{1}H NMR spectrum of **3** in $CDCl_3$ showed 12 distinct aromatic signals in the range δ 6.49−9.38 and 4 different doublet CH_2N resonances at δ 4.20, 4.97, 5.35, and 5.49 for ligand **L1**. The methyl and methylene groups of the cycloneophyl ligand each gave 2 distinct resonances. These NMR data, which were similar for the other complexes **4**−**6**, indicate a single octahedral palladium(IV) complex with no symmetry. While the NMR data did not reveal the stereochemistry, it was determined by X-ray diffraction of complexes **3** and **5**, which are coordinated by the hydroxyl-substituted ligand **L1**. The octahedral geometry was confirmed, and in both cases, the observed isomer exhibits a *trans* disposition of the coordinated iodide to the tertiary amine donor of **L1** (Figures 2 and 3). On the basis of the usual polar mechanism of oxidative addition of halogens to Ir(I) or Pt(II),[32−36] we had instead expected the palladium(IV) product to be formed from **1** by formal addition of I$^+$ above the plane with coordination of the free pyridyl group below the plane to give an isomer with mutually *trans* iodide and pyridyl groups. The difference suggests that the initial oxidative addition product

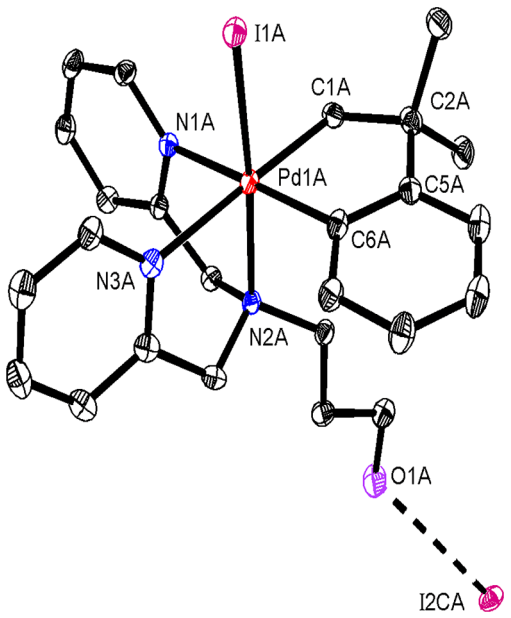

Figure 2. Structure of complex **3** (showing 30% probability ellipsoids) obtained from the cocrystal [**3**·7·Me_2CO]. Selected bond distances: Pd(1A)−I(1A) 2.5785(9); Pd(1A)−N(1A) 2.150(4); Pd(1A)−N(2A) 2.197(4); Pd(1A)−N(3A) 2.229(5); Pd(1A)−C(1A) 2.072(5); Pd(1A)−C(6A) 1.994(6) Å; H-bond distance O(1A)···I(2CA) 3.54(1) Å.

isomerizes to give **3**−**6**, the thermodynamically preferred structures.

Crystallization of complex **3** from acetone/pentane at room temperature occurred with partial decomposition to the palladium(II) complex **7** to give cocrystals of **3** and **7** as the acetone solvate (**3**·7·Me_2CO). The structure of complex **3** confirms that **L1** acts as a *fac*-tridentate ligand and that the iodide ligand is *trans* to the amine donor while the two pyridyl donors are *trans* to carbon donors of the cycloneophyl group (Figure 2). The ligand hydroxyl group in **3** is not coordinated, but it is hydrogen-bonded to an iodide anion.

Crystals of complex **5**, formed as an acetone solvate, were grown from acetone/acetonitrile at low temperature (−15 °C) to avoid decomposition (Figure 3). There were two independent molecules in the lattice, which both have the same stereochemistry as complex **3**, with the amine donor *trans* to halide (cf. Figure 2), but were refined as enantiomers. Again, the ligand hydroxyl group was hydrogen-bonded to the uncoordinated halide anion (bromide in this case).

The palladium(II) complexes **7**−**10** were also fully characterized by NMR and IR spectroscopies and ESI-MS. The NMR spectra gave simpler signatures in comparison to the precursor complexes **3**−**6**, which is consistent with a more symmetric, C_s, structure. For example, complex **7** gave only one set of pyridyl resonances and equivalent 2-pyridylmethyl groups. A single crystal of each of **7**−**10** was obtained and analyzed by X-ray crystallography (Figure 4). The expected square-planar geometry is observed with minimal distortion[37] (τ^4 = 0.11−0.15). In all complexes, the ligand **L1** or **L2** acts as a *mer*-tridentate ligand, binding through the three nitrogen atoms. The Pd−N_{py} and Pd−N_{amine} distances are similar for the set. In complexes **7** (a component of the cocrystal **3**·7·Me_2CO) and **9**, the ligand hydroxyl group is hydrogen-bonded to the uncoordinated iodide or bromide anion, respectively.

https://dx.doi.org/10.1021/acs.organomet.0c00615
Organometallics XXXX, XXX, XXX−XXX

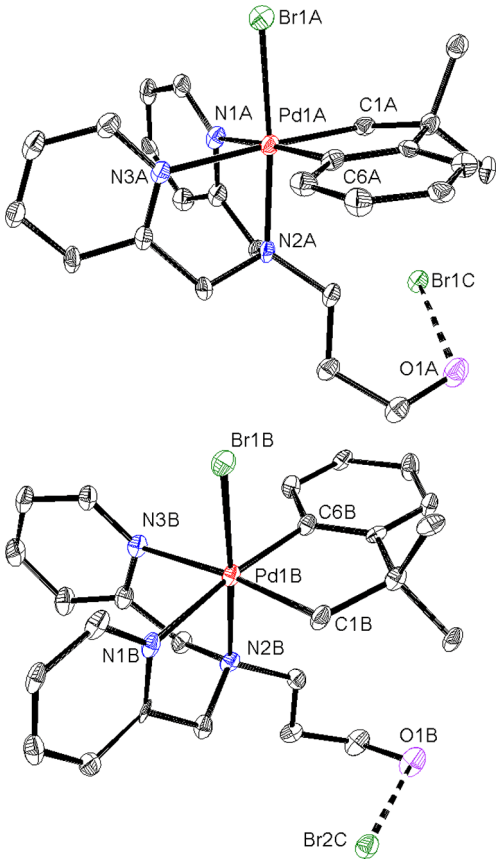

Figure 3. Structure of complex **5** showing 30% probability ellipsoids for the two independent molecules. Selected bond distances (Å): molecule **A**, Pd(1A)−I(1A) 2.420(2); Pd(1A)−N(1A) 2.171(12); Pd(1A)−N(2A) 2.121(12); Pd(1A)−N(3A) 2.203(12); Pd(1A)−C(1A) 2.075(13); Pd(1A)−C(6A) 1.985(15); molecule **B**, Pd(1B)−I(1B) 2.4272(19); Pd(1B)−N(1B) 2.154(12); Pd(1B)−N(2B) 2.147(12); Pd(1B)−N(3B) 2.206(12); Pd(1B)−C(1B) 2.049(12); Pd(1B)−C(6B) 1.996(15).

Palladium Complexes from Reaction with Methyl Iodide. The reaction of methyl iodide with complex **1** at room temperature gave the palladium(II)−alkyl complex **13** that exhibits *mer* coordination of **L1** (Scheme 5). This is the expected product if oxidative addition of **1** by MeI gives intermediate **11**, which undergoes reductive elimination by selective coupling of the methyl and aryl group ($C(sp^3)$–$C(sp^2)$ bond formation). The presence of palladium(IV) intermediate **11** was supported by low-temperature NMR spectroscopy (*vide infra*). The ^{1}H NMR spectrum of the final palladium(II) product **13** (Figure 5) contained only one set of resonances for the pyridyl groups and gave singlet resonances for the $PdCH_2$, CMe_2, and Me-C_6H_4 groups with relative intensities 2:6:3, as expected for a complex with C_s symmetry. These data are clearly not consistent with the palladium(IV) complex **11** or with potential products of reductive elimination by coupling of methyl and CH_2 groups ($C(sp^3)$–$C(sp^3)$ coupling) or by coupling of the CH_2 and aryl groups which would give the benzocyclobutane derivative **CB** (compare Scheme 2) and a methylpalladium(II) complex. The reaction of **1** with CD_3I gave the corresponding complex **13-*d*$_3$**. The ^{1}H NMR spectrum of **13-*d*$_3$** was identical with that **13**, except without a singlet at 2.66 ppm that corresponds to a methyl group. Rather, a broad signal was observed at a similar chemical shift value in the ^{2}H NMR spectrum (Figure 5). This

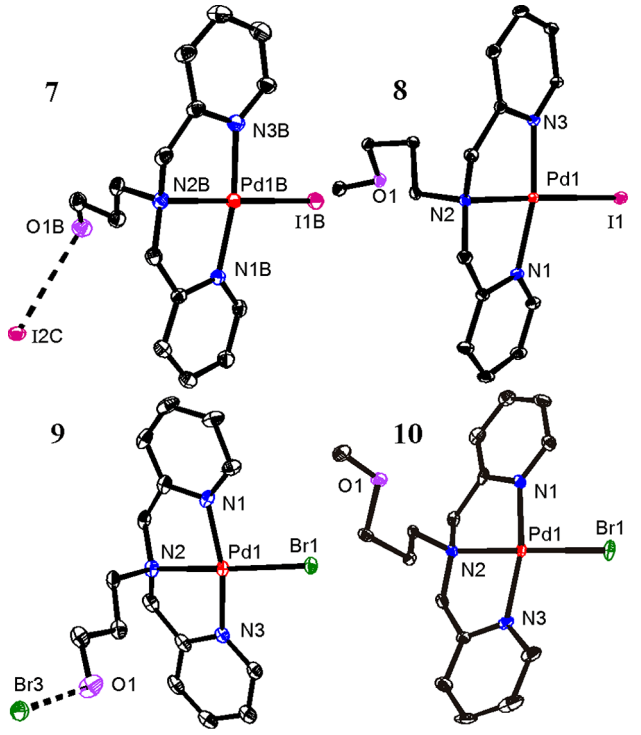

Figure 4. Structures of complexes **7**−**10**. Selected distances: complex **7**, Pd(1B)−I(1B) 2.5928(10); Pd(1B)−N(1B) 2.025(5); Pd(1B)−N(2B) 2.055(5); Pd(1B)−N(3B) 2.037(5) Å; complex **8**, Pd(1)−I(1) 2.5911(19); Pd(1)−N(1) 2.028(2); Pd(1)−N(2) 2.041(2); Pd(1)−N(3) 2.017(2) Å; complex **9**, Pd(1)−Br(1) 2.4101(8); Pd(1)−N(1) 2.026(5); Pd(1)−N(2) 2.014(5); Pd(1)−N(3) 2.034(5) Å; complex **10**, Pd(1)−Br(1) 2.4282(12); Pd(1)−N(1) 2.024(5); Pd(1)−N(2) 2.038(5); Pd(1)−N(3) 1.993(5) Å. τ^4 values: **7**, 0.13; **8**, 0.15; **9**, 0.11; **10**, 0.11.

Scheme 5. Reaction of Complexes 1 and 2 with Methyl Iodide to Give Proposed Intermediate Palladium(IV) Complexes 11 and 12 and Final Reductive Elimination Palladium(II) Products 13 and 14[a]

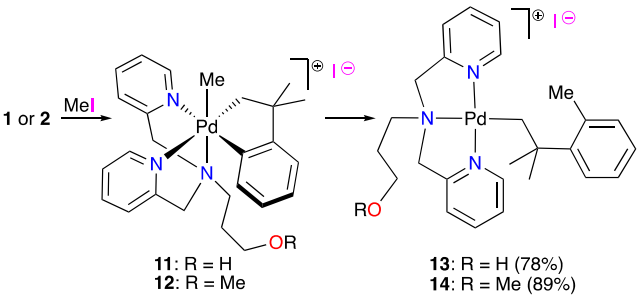

[a]Isolated yields are given in parentheses.

confirms the assignment of the aryl-bound methyl as originating from the MeI oxidant and that no evidence for a $C(sp^3)$–$C(sp^3)$ coupling product was observed. The reaction of methyl iodide with **L2** complex **2** occurred similarly to give **12** as an intermediate (*vide infra*) and palladium(II)−alkyl complex **14** as the final product (Scheme 5). The spectroscopic data for **14** were closely analogous to those of **13**.

The reaction of **1** with MeI or CD_3I was also carried out at low temperature in order to detect the proposed palladium(IV) intermediate, **11**. The reagents were mixed at −30 °C,

https://dx.doi.org/10.1021/acs.organomet.0c00615
Organometallics XXXX, XXX, XXX−XXX

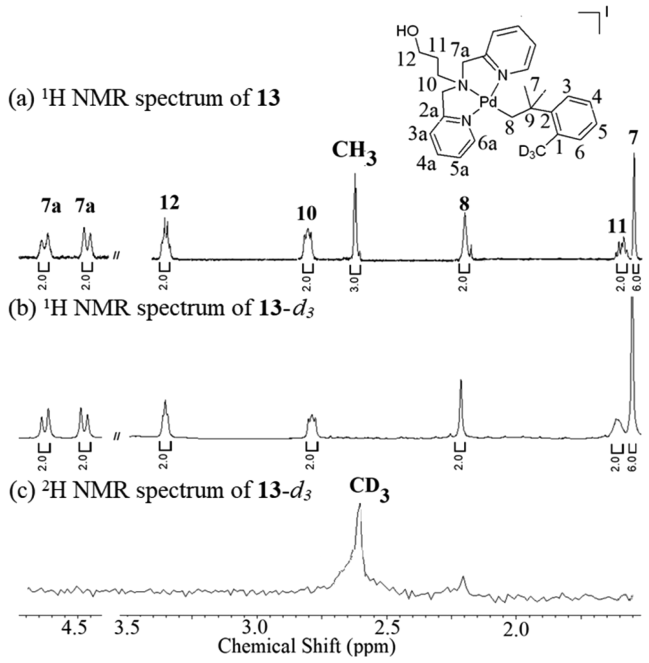

Figure 5. NMR spectra of complex **13** and **13-d_3**: (a) ^{1}H NMR spectrum of **13** in CD_2Cl_2; (b) ^{1}H NMR spectrum of **13-d_3** in CD_2Cl_2; (c) ^{2}H NMR spectrum of **13-d_3** in CH_2Cl_2.

and NMR spectra were recorded on warming to room temperature. The reaction was slow at −30 °C, but peaks for complex **1** decayed and were replaced by peaks characteristic of a palladium(IV) complex at 0 °C. The ligand and cycloneophyl resonances were similar to those for **3** and **5**; thus, although the data do not unambiguously define the stereochemistry, the related structure **11** is suggested for this intermediate. The methylpalladium resonance of the intermediate **11** was observed as a singlet at δ 1.91, ca. 0.6 ppm upfield of the aryl-substituted methyl group in **13** that forms after C−C bond formation. At temperatures above 0 °C, reductive elimination from **11** occurred, since the peaks for the palladium(IV) complex were replaced by those for the palladium(II) product **13**. No other set of signals was observed, which indicates that the reaction occurred selectively. The similar reaction at low temperature of complex **2** gave the palladium(IV) intermediate **12**, which had a thermal stability similar to that of **11** and which decomposed by warming to room temperature to give **14** (Scheme 5).

There have been several studies of selectivity in C−C coupling reactions at palladium(IV)[7−14,38,39] or platinum(IV)[8−10,14,38,40−46] centers, though few[8] of them involve the cycloneophyl group. Most of the known reactions proceed after dissociation of an ancillary ligand to give a five-coordinate intermediate.[32−35,44−49] In simple dimethyl(aryl) derivatives, there is a preference for C(sp^3)−C(sp^3) coupling to give ethane rather than C(sp^3)−C(sp^2) coupling to give the corresponding methylarene.[39,40] However, if the aryl group is part of a cyclometalated chelate group, there is usually a kinetic preference for methyl−aryl C(sp^3)−C(sp^2) coupling.[41−43] The reactivity of **11** and **12** falls into this pattern, with the selectivity for C(sp^3)−C(sp^2) coupling rationalized in terms of the favorable orientation of the plane of the aryl group roughly orthogonal to the methylpalladium(IV) bond, which allows facile access to the transition state for methyl−aryl group coupling.[39−43]

Organic Products from the Reductive Elimination Reactions of Complexes 3−6. Previous studies of reductive elimination from cycloneophylpalladium(IV) complexes have shown a high degree of selectivity, though the reactions may occur by C−C coupling to give the cyclobutane derivative **CB** or by CH_2−X or Ar−X coupling to give organopalladium(II) products (Schemes 1 and 2).[19−29,50] However, the reductive elimination reactions from the palladium(IV) complexes **3−6** were not very selective (Scheme 6 and Table 1). The

Scheme 6. Mixture of Organic Products Detected from Reductive Elimination from Complexes 3−6 (X = I from 3 and 4, X = Br from 5 and 6)

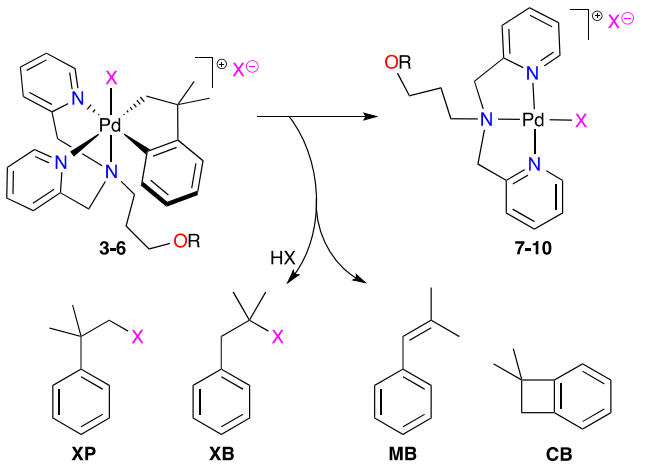

decomposition of **3−6** in $CDCl_3$ solution gave the cyclobutane derivative **CB** by C−C coupling in yields ranging from 5 to 30% (Table 1). The other observed products are less easily explained. The neophyl halide product, **XP** (Scheme 6), is expected to be formed by X−CH_2 coupling but also with protonolysis of the arylpalladium bond. This unanticipated protonolysis step is also required in the formation of the products **XB** and **MB** (Scheme 6), but with an additional step involving a "cation-like" neophyl rearrangement with phenyl group migration.[51] The neophyl halides are stable to substitution under the mild conditions used in this work (most rearrangement studies have involved the more reactive triflates or tosylates);[51] thus, the neophyl rearrangement must occur while the organic group is still bound to palladium.[26,29,52] The reaction stoichiometry indicates that an additional 1 equiv of HX is required to form **XP** and **XB**. By using dry solvent, no **XP** or **XB** was formed and **CB** and **MB** yields increased (Table 1), indicating that adventitious water is the source of the additional proton equivalent. The reaction of complex **4** in $CDCl_3$ saturated with D_2O gave the mixture of organic products **XP**-d_1, **XB**-d_1 (X = I), and **MB**-d_1, which are expected to be formed if water is involved in the protonolysis step. In the ^{2}H NMR spectrum of the reaction mixture, two resonances were resolved at δ 7.37 and 7.25, which confirms deuterium incorporation at an aryl carbon atom. The aryl resonances for **XP**, **XB**, and **MB** all overlap in the narrow range δ 7.14−7.35 in the ^{1}H NMR spectrum; thus, it was only possible to confirm the incorporation of deuterium atoms but not to confirm their expected *ortho* positions. The product ratios (Table 1 and Figure S66) are affected by both the ligand (**L1** vs **L2**) and the halide (Br vs I). **XP** is the major product with **L1** complexes **3** and **5**, but **MB** has higher yields with **L2**

https://dx.doi.org/10.1021/acs.organomet.0c00615
Organometallics XXXX, XXX, XXX−XXX

Table 1. Observed Products after Reductive Elimination from Complexes 3−6 in $CDCl_3$ Solution[a]

reagent	X	Pd product (%)[b]	organic product (%) CB	XP	XB	MB	CB:(XP + XB + MB)
3	I	**7** (87)	5	37	28	20	1:17
4	I	**8** (93)	5	25	8	48	1:16
4a[c]	I	**8a** (80)	30	13		25	1:1.3
5	Br	**9** (90)	28	50		9	1:2.1
6	Br	**10** (84)	10	24		50	1:7.4
6[d]	Br	**10** (80)	30			61	1:2

[a]Conditions: 50 °C, 7.5 h, unless otherwise specified. [b]Isolated yield for palladium products and *in situ* NMR yields for organic products. [c]60 h reaction time. [d]In dry $CDCl_3$ solution.

complexes **4** and **6**. This may suggest that the hydroxyl group of **L1** assists in intermolecular proton shuttling from H_2O to the neophyl ligand. The tetrafluoroborate salt **4a** gave a higher yield of **CB** in comparison to the corresponding iodide salt **4**. This is consistent with the expectation that uncoordinated iodide is involved in the formation of **XP**, **XB**, and **MB**.

From the initial product analyses (Table 1) and from literature precedents,[19−23,28,29,44−49] the reaction sequence shown in Scheme 7 (*NNN* = **L1**, **L2**; X = Br, I) was

Scheme 7. Potential Pathway for the Reductive Elimination Reactions

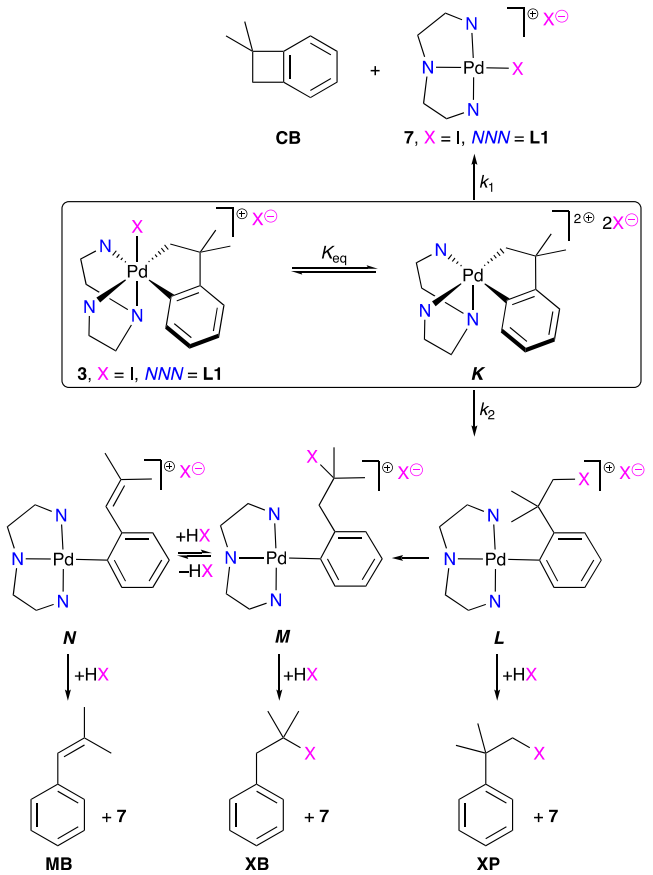

considered as a working hypothesis. The reductive elimination steps are likely to occur by way of a five-coordinate intermediate formed by ligand dissociation from the palladium(IV) complex **3** (used as an example of **3**−**6**). If the dissociating ligand is iodide, this five-coordinate intermediate is the dication ***K*** (Scheme 7). Complex ***K*** can undergo reductive elimination with C−C coupling to give **CB**, followed by rapid coordination of iodide to give **7**. Alternatively, ***K*** can undergo nucleophilic attack by iodide at the CH_2 group to give Pd−Ar complex ***L***, which could lead to each of the remaining organic products, **XP**, **XB** ,and **MB**. Protonolysis of the aryl−palladium bond in ***L*** would give **XP** (X = I) and palladium(II) complex **7**. Alternatively, halide abstraction by the cationic palladium in ***L*** could give an intermediate or incipient cation on the neophyl group, which is known to undergo rearrangement.[29,51,53−55] Irreversible phenyl migration and rehalogenation of the neophyl would afford intermediate ***M*** (Scheme S1), which would give **XB** and **7** following protonolysis. Alternatively, the organic ligand of ***M*** could undergo a dehydrohalogenation to give an alkene in ***N***. Protonolysis with the released HX would afford **7** and **MB**. Organic products **XB** and **XP** were not observed under dry solvent conditions, where the only source of HX was from the formation of ***N***. Therefore, protonolysis of ***N*** likely occurs rapidly, before the released HX diffuses away to react with ***M*** or ***L***.

Several further experiments were carried out to test the validity of the mechanism in Scheme 7. The decomposition of complex **3** in $CDCl_3$ solution was monitored by ^{1}H NMR spectroscopy in an attempt to detect the proposed intermediates ***L***, ***M***, and ***N***. One intermediate was detected as the reaction progressed; its concentration was always low, but it was tentatively identified as ***M*** by its ^{1}H NMR spectrum. The 2-pyridylmethylene groups were equivalent (e.g., δ-(CH^aH^b) 5.10, 4.47, each 2H, ^2J(HH) = 15 Hz, H7a and H7b), while the neophyl group gave the expected singlet resonances for the CH_2 and CMe_2 groups at δ 1.63 and 1.96, respectively. By comparison, the CH_2I signal in intermediate ***L*** would be expected at a higher chemical shift value due to deshielding by the halide. If Scheme 7 is correct, the ratio of **CB** to the sum of the other products (**XP**, **XB**, **MB**) should be given by the ratio $k_1/k_2[X^-]$, where k_1 is the first-order rate constant for reductive elimination from ***K*** to give **CB** and k_2 is the second-order rate constant for formation of intermediate ***L*** by halide attack on ***K***. These ratios, **CB**:(**XP** + **XB** + **MB**), were approximately 1:7, 1:16, and 1:6 for reactions of **4** in benzene, chloroform, and methanol, respectively, showing no correlation with solvent polarity.[56] In methanol saturated with sodium iodide, the formation of **CB** was suppressed, as expected from Scheme 7. There is an analogy with the mechanistic study by the Goldberg group on the decomposition of [$PtIMe_3$(dppe)] (dppe = $Ph_2PCH_2CH_2PPh_2$).[45] This reductive elimination reaction was shown to occur from the five-coordinate intermediate [$PtMe_3$(dppe)]$^+I^-$ by competitive C−C coupling (to give ethane and [PtIMe(dppe)]) and C−I coupling (to give methyl iodide and [$PtMe_2$(dppe)]),

https://dx.doi.org/10.1021/acs.organomet.0c00615
Organometallics XXXX, XXX, XXX−XXX

and the ethane formation was suppressed in the presence of excess iodide. The ratio **CB**:(**XP** + **XB** + **MB**) for decomposition was 1:16 for complex **4**, which has a noncoordinating iodide anion, but 1:2.3 for complex **4a**, which has a tetrafluoroborate anion (Table 1). This again indicates that free iodide favors formation of **XP**, **XB**, and **MB** over **CB**. Reductive elimination from **4a** takes approximately 10 times longer than **4** to achieve a similar conversion (Table 1); thus, qualitatively the presence of noncoordinating iodide leads to much faster rates. All of these data are at least consistent with the mechanism of Scheme 7.

Kinetic Studies. Kinetic studies of the reductive elimination reactions were carried out using UV−visible spectroscopy to monitor the rates. The proposed mechanism of Scheme 7 is complex, but the relevant parts of the UV−visible spectra are dominated by the palladium cations (reagent **3** and product **7** in Scheme 7); therefore, the overall rate of reductive elimination can be measured. Under conditions where there is a pre-equilibrium between **3** and ***K*** (Scheme 7, equilibrium constant K_{eq}), the concentration of ***K*** will be given by $[\boldsymbol{K}] = K_{eq}[\mathbf{3}]/[X^-]$. The overall steady-state rate is then expected to be given by the expression $-d(\mathbf{3})/dt = (k_1 + k_2[X^-])[\boldsymbol{K}] = K_{eq}(k_1 + k_2[X^-])[\mathbf{3}]/[X^-] = k_{obs}[\mathbf{3}]$, where $k_{obs} = K_{eq}k_1/[X^-] + K_{eq}k_2$. The halide concentration is expected to decrease during the reaction as the products **XP** and **XB** are formed; thus, good first-order kinetics cannot be expected. Nevertheless, first-order plots of $\ln[A - A_\infty]/[A_0 - A_\infty]$ vs time were approximately linear at early time points and the values of k_{obs} can at least be taken as a measure of reactivity.

A series of spectra were obtained for the reductive elimination from complex **3** in chloroform solution at 50 °C. Along with the first-order plot using changes in the absorbance at 425 nm (Figure 6), a summary of the k_{obs} values is given in Table 2. The reactions using **3** and **4** were each carried out in three solvents of different polarity: namely, benzene, chloroform, and methanol (dielectric constant ε = 2.2, 4.8, 33.6, respectively). The values of k_{obs} for reaction of complex **3** in benzene, chloroform, and methanol were 0.0162(5), 0.0211(2), and 0.020(1) min^{-1} and for **4** they were

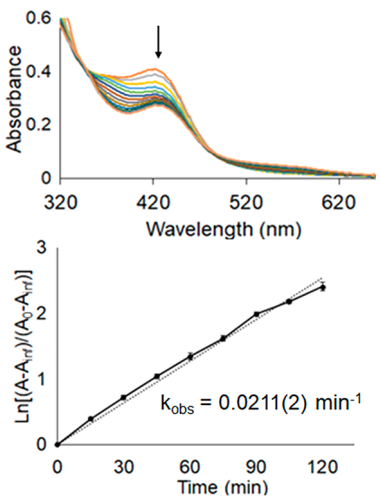

Figure 6. (top) UV−visible absorption spectra of complex **3** in chloroform (8.33×10^{-3} M, 50 °C) during the reductive elimination reaction where the absorbance centered at 425 nm decreases with time. (bottom) Corresponding first-order plot of $\ln[A - A_\infty]/[A_0 - A_\infty]$ versus time for the initial part of the reaction.

Table 2. Observed First-Order Rate Constants for the Reductive Elimination Reactions[a]

complex	additive	solvent	ε[b]	k_{obs} (min^{-1})
3		C_6H_6	2.2	0.0162(5)
3		$CHCl_3$	4.8	0.0211(2)
3		CH_3OH	33.6	0.0200(1)
3	NaI[c]	CH_3OH	33.6	0.0199(1)
3	pyridine[c]	CH_3OH	33.6	0.0212(1)
4		C_6H_6	2.2	0.0170(1)
4		$CHCl_3$	4.8	0.0190(1)
4		CH_3OH	33.6	0.0190(1)
4a		$CHCl_3$	4.8	0.0028(3)
5		$CHCl_3$	4.8	0.0158(2)

[a][Pd] = 8.33×10^{-3} M; see the Experimental Section for additional details. [b]Dielectric constant. [c][NaI] or [py] = 8.33×10^{-2} M.

0.017(1), 0.019(1), and 0.019(1) min^{-1}, respectively. There is very little difference in these values; thus, clearly the effect of solvent polarity is small and the different ligand substituents (OH in **3** and OMe in **4**) also have very little effect on the overall rate of reductive elimination. Similarly, the bromide derivative **5** reacts at a rate similar to that of the iodide derivative **3**, with k_{obs} = 0.016(2) and 0.0211(2) min^{-1}, respectively, at 50 °C in chloroform solution. The reaction of complex **3** in methanol solution at 50 °C was also monitored in the presence of a 10-fold excess of sodium iodide or free pyridine, but neither had a significant effect on the rate of reaction (Table 2). The bromo derivative **5** reacted somewhat more slowly than the iodo derivative **3** in chloroform solution (k_{obs} = 0.0211(2) and 0.0158(2) for **3** and **5**, respectively). This suggests that the identity of the halide has a minimal effect on the overall rate. However, the greater selectivity of **3** vs **5** for C−X over C−C bond formation (**CB**:(**XP** + **XB** + **MB**), = 1:17 (**3**), 1:2 (**5**)) suggests that the relative barriers for the two routes (***K*** → ***L*** and ***K*** → **7**, respectively) are influenced by the nature of the halide. The only case in which a major difference in rate was observed was in the decomposition of **4** and the BF_4^- analogue **4a** in chloroform at 50 °C, with k_{obs} = 0.0211(2) and 0.0028(3) min^{-1}, respectively, with **4** reacting about 7 times faster than **4a**. This shows clearly that the reaction does not occur by direct intramolecular reductive elimination from complex **3**, since in that case the rates for **4** and **4a** should be very similar. Overall, the kinetic data are in accord with qualitative observations made when similar reactions were monitored by ^{1}H NMR spectroscopy (Tables 1 and 2) and are consistent with the proposed mechanism shown in Scheme 7.

Computational Studies. In order to gain more insight into the selectivity of the reactions, some calculations were carried out using density functional theory (BLYP functional, scalar correction for relativity).[57,58] One limitation is that the sequence of reactions begins with neutral palladium(II) reagents, but given the ionic palladium(IV) and palladium(II) products and given the complexity of the compounds, we have not attempted to model the resulting changes in solvation effects. Instead, we have generally made only gas-phase calculations with complex **1** as the reagent and have modeled the ionic products as zwitterions, with the iodide ion hydrogen bonded to the hydroxyl substituent of the ligand. Naturally, this methodology will not give accurate data for the step in which the ionic compounds are first formed, but it should give more reliable data for compounds with like charges. As an

https://dx.doi.org/10.1021/acs.organomet.0c00615
Organometallics XXXX, XXX, XXX−XXX

example, the potential products from reactions of complex **1** with methyl iodide are shown in Scheme 8, while calculated

Scheme 8. Three Potential Modes of Reductive Elimination from Complex 11 with C−C Bond Formation

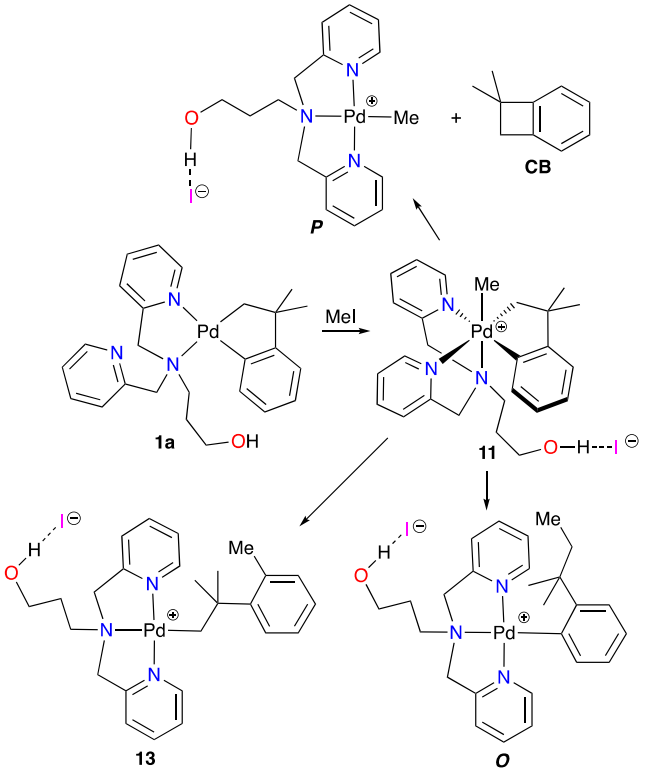

structures and relative energies with respect to **1a** and MeI are shown in Figure 7. The initial reaction of **1a** with methyl iodide is calculated to be unfavorable (ΔE = +30 kJ mol^{-1}), no doubt because of the poor modeling of the solvation of the ions. The three potential routes for reductive elimination from

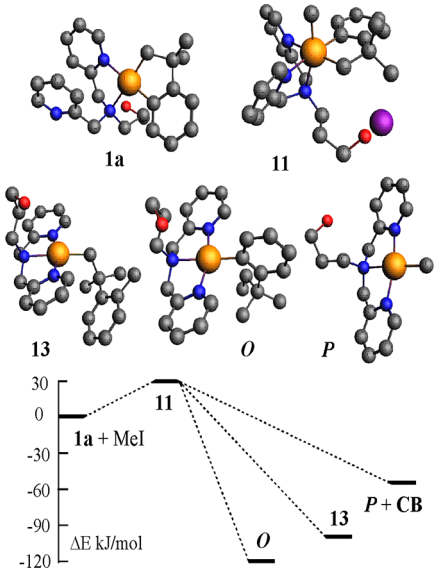

Figure 7. Calculated structures of complexes shown in Scheme 8 (the iodide ion is not shown in the Pd(II) complexes for clarity) and the relative energies (kJ mol^{-1}) with respect to **1a** + MeI.

11 with C−C bond formation occur with no change in charges, and so the relative energies with respect to **11** should be more reliable. The potential products are **13** formed by methyl−aryl coupling, ***O*** formed by methyl−alkyl coupling, and ***P*** and **CB** formed by alkyl−aryl coupling (alkyl represents the Pd−CH_2 group of the metallacycle) (Scheme 8). The formation of ***P*** and **CB** is clearly the least favorable (ΔE = −54 kJ mol^{-1}, Figure 7), as expected in view of the ring strain of the **CB** product. The calculations predict that the formation of ***O*** (ΔE = −123 kJ mol^{-1}) is more favorable than the formation of the observed product **13** (ΔE = −106 kJ mol^{-1}). We have not calculated transition states, but the calculation is consistent with the selective formation of **13** being determined by kinetic and not thermodynamic control.[41−43]

Figure 8 shows the calculated structures and relative energies for products and potential products from reductive elimination

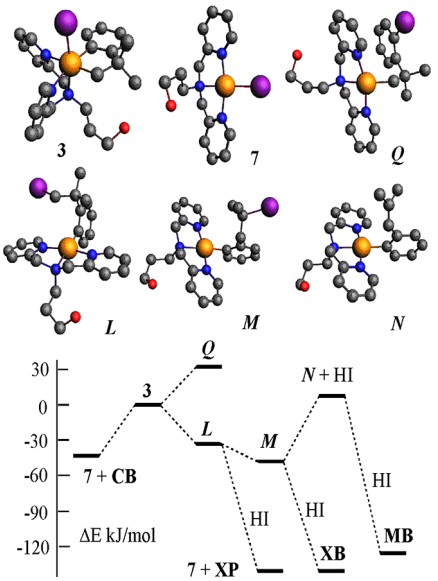

Figure 8. Calculated structures of cationic complexes shown in Scheme 7 and the relative energies (kJ mol^{-1}) with respect to complex **3**.

from the iodopalladium(IV) complex **3** (Scheme 7). Again, all of the palladium compounds are cationic and they are treated as zwitterions in the calculations. This reaction could occur initially by C−C coupling to form **7** and **CB**, I−CH_2 coupling to form ***L***, or I−Ar coupling to form ***Q*** (Figure 8). The aryl−iodide coupling to give complex ***Q*** is calculated to be unfavorable, and ***Q*** is not observed experimentally, but the other two routes are favorable and the ^{1}H NMR spectroscopy evidence indicates that they both occur. The organic products **XP**, **XB** ,and **MB** are expected to form by protonolysis of ***L*** or the products of its neophyl rearrangement ***M*** and ***N***. These products are at considerably lower energy than the cyclobutane derivative **CB**, but the ratio of **CB** to the combined products **XP**, **XB**, and **MB** will be controlled by the initial reductive elimination steps to form **7** and **CB** or to form ***L***, and these are competitive (Figure 8). However, for **3** the experimental **CB**:(**XP** + **XB** + **MB**) ratio of 1:17 suggests that reductive elimination to give ***L*** is preferred by far. These data suggest that the selectivity is more likely to be under kinetic rather than thermodynamic control.

One remaining puzzle is why the oxidative addition of iodine occurs selectively to form complex **3** rather than its isomers **3a**

https://dx.doi.org/10.1021/acs.organomet.0c00615
Organometallics XXXX, XXX, XXX−XXX

and **3b** (Figure 9). The palladium(II) isomers **1a** and **1b** (Scheme 3) are chiral, and in both cases attack by iodine is also

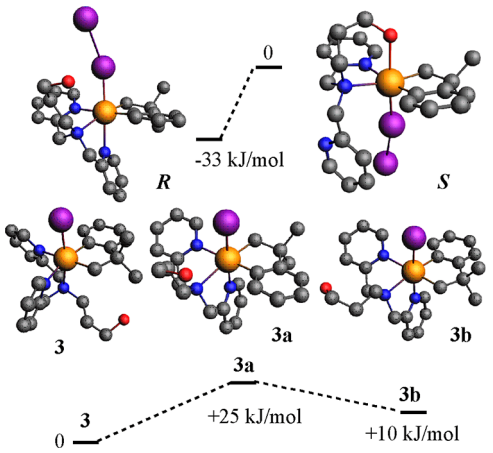

Figure 9. Calculated structures of isomers of **3** and possible intermediate iodine complexes ***R*** and ***S*** and their relative energies (kJ mol^{-1}).

expected to result in coordination of a third donor group of **L1** to the site trans to initial I_2 coordination.[34,35] Since iodine attack could occur on either side of the square plane of the palladium(II) precursor, the expected products from attack on **1a** are either ***R***, with a *trans* 2-pyridylmethyl group, or ***S***, with a *trans* 3-hydroxypropyl group. The calculations show that ***R*** is ca. 30 kJ mol^{-1} lower in energy than ***S***. The κ^3-*N,N′,N″* coordination mode of **L1** in ***R*** is consistent with the coordination mode of the observed palladium(IV) products. If the final product were to be formed by kinetic control, ***R*** would be expected to give isomer **3a** that forms directly following I–I bond cleavage. Similarly, **1b** would form an isomer of ***R*** that would give **3b**. However, neither **3a** or **3b** is observed experimentally, which suggests that the final product is formed under thermodynamic control. Indeed, the experimentally observed complex **3** is calculated to be more stable than either **3a** or **3b**, though the differences are small (Figure 9).

CONCLUSION

The cycloneophylpalladium(IV) complexes reported above contain flexible tridentate ligands that stabilize the palladium(IV) oxidation state to an extent that allows their isolation (or characterization at reduced temperature for the methylpalladium(IV) complexes), but not so much that the compounds require forcing conditions to initiate reductive elimination. The most selective reductive elimination is observed for the methylpalladium(IV) complexes **11** and **12**, which give only Me–Ar bond formation at about 0 °C in solution (Scheme 5). No $C(sp^3)$–$C(sp^3)$ or C–X bond formation was observed with these complexes, and computations suggest that the product selectivity is due to a kinetic preference for Me–Ar vs Me–alkyl bond formation. The halogen palladium(IV) complexes **3–6** are sufficiently stable to be isolated, but they slowly undergo reductive elimination in solution to give the palladium(II) products [PdX(κ^3-*N,N′,N″*-**L**)]X (X = Br, I). The organic products revealed that C–X coupling selectively occurs with the sp^3 carbon, but a mixture of compounds was formed due to facile neophyl rearrangement and protonolysis steps. Additionally, a C–C bond formation cyclobutane product was formed due to competition with C–X bond formation at the rate-limiting reductive elimination step (Scheme 7). The slow reductive elimination reaction of **4a** (BF_4^- counteranion) in comparison to **4** (I^- counteranion) suggests that the reductive elimination occurs by a mechanism in which **3–6**, $[PdX(CH_2CMe_2C_6H_4)(\kappa^3\text{-}N,N',N''\text{-}L)]^+$ (X = Br, I), undergoes reversible halide dissociation to give the five-coordinate intermediate $[Pd(CH_2CMe_2C_6H_4)(\kappa^3\text{-}N,N',N''\text{-}L)]^{2+}$. This intermediate can then undergo intramolecular reductive elimination with CH_2–Ar bond formation, to give the cyclobutane derivative **CB** and $[PdX(\kappa^3\text{-}N,N',N''\text{-}L)]^+$ (**7–10**), or by halide attack on the Pd–CH_2 group to give initially $[Pd(2\text{-}C_6H_4CMe_2CH_2X)(\kappa^3\text{-}N,N',N''\text{-}L)]^+$, which then undergoes the neophyl rearrangement and/or protonolysis of the aryl–palladium(II) bond to give a mixture of organic products. While this mixture of products is undesirable in the context of catalysis, it is encouraging that intermolecular halide attack occurs exclusively at the sp^3 carbon center. The complexes with ligands **L1** and **L2** have similar reactivities in these reactions, indicating that the hydroxyl substituent in **L1** plays only a minor role in the rate-determining steps. The ligand does affect the selectivity, dominantly among the various CH_2–X reductive elimination products. The work is significant in giving new insights into the reactivity and mechanism in palladium(II)–palladium(IV) cycles that are important in several catalytic reactions.

EXPERIMENTAL SECTION

Reagents and General Procedures. All reactions were carried out in air at room temperature, unless otherwise noted. For those reactions that were conducted under a nitrogen atmosphere, standard Schlenk or glovebox techniques were used. All solvents used for air- and moisture-sensitive reactions were purified using an Innovative Technologies 400-5 Solvent Purification System (SPS) and were stored over activated 4 Å molecular sieves. NMR spectra were recorded using a Varian 600 spectrometer. ^1H and ^{13}C chemical shifts were referenced internally to solvent (residual signal for ^1H), where the chemical shift was set to appropriate values relative to TMS at 0.00 ppm. Chemical shifts are reported relative to trifluorotoluene for ^{19}F NMR. Complete assignments of each compound were aided by the use of ^1H–^1H gCOSY, ^1H–$^{13}C\{^1H\}$ HSQC, and ^1H–$^{13}C\{^1H\}$ HMBC experiments and are reported using the labeling scheme in Chart 1 and Figures 1 and 4. For ^2H NMR experiments, the ^2H

Chart 1. NMR Labels for Pd(IV) Complexes 3–6

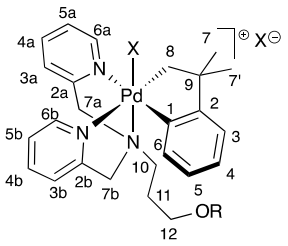

chemical shift was referenced externally to the ^2H peak of CD_2Cl_2 ($\delta(^2H)$ 5.34). The DFT calculations were carried out using methods implemented in ADF-2019, with minima confirmed by vibrational analysis.[57,58] The BLYP functional, which has been widely used in studies of energetics and mechanism in organometallic chemistry, was used, with a double-ζ basis set and first-order scalar relativistic corrections for platinum. Details of the calculated structures and energies are given in the Supporting Information. Commercial reagents were used without further purification. The complexes $[PdCl_2(COD)]$,[59,60] $[Pd(CH_2CMe_2C_6H_4)(COD)]$,[25] and [Pd-

https://dx.doi.org/10.1021/acs.organomet.0c00615
Organometallics XXXX, XXX, XXX–XXX

$(CH_2CMe_2C_6H_4)(\kappa^2\text{-}N,N'\text{-}\mathbf{L1})]$ (**1**)[29] and ligands *N,N*-bis(pyrid-2-ylmethyl)-*N*-(2-hydroxyethyl)amine (**L1**)[30] and *N,N*-bis(pyrid-2-ylmethyl)-*N*-(2-methoxyethyl)amine (**L2**)[31] were synthesized according to the literature procedures. Elemental analyses were performed by Laboratoire d'Analyze Élémentaire de l'Université de Montréal. Organic products were analyzed using a Shimadzu GCMS-QP2010 Ultra GC instrument with a DB-5 column. Infrared spectra were collected on solid samples using a PerkinElmer UATR TWO FT-IR spectrometer. UV−visible spectra were collected using an Agilent Technologies Cary 8454 UV−visible spectrometer. MALDI-TOF mass spectra were collected using an AB Sciex 5800 TOF/TOF mass spectrometer using anthracene as the matrix in a 20:1 matrix:substrate molar ratio.

Synthesis of $[Pd^{II}(CH_2CMe_2C_6H_4)(\kappa^2\text{-}N,N'\text{-}L2)]$ (2). Under N_2, a solution of 3-methoxy-*N,N*-bis(pyridin-2-ylmethyl)propan-1-amine (**L2**; 0.117 g, 0.432 mmol) in dry THF (15 mL) was added to a stirred solution of $[Pd(CH_2CMe_2C_6H_4)(COD)]$ (0.150 g, 0.433 mmol) in dry THF (25 mL) cooled to −65 °C. The mixture was stirred and slowly warmed to room temperature over 4 h. Upon removal of the solvent under reduced pressure, a brown oil was formed which was washed with hexanes (20 mL) and ether (10 mL). The oil was dried under vacuum, to give **2** (0.164 g, 0.322 mmol, 75%). ^{1}H NMR (CD_2Cl_2, 600 MHz, 25 °C): δ 8.45−8.55 (m, 2H, H6b and H6a), 7.64−7.68 (m, 3H, H4a, H5b, and H4b), 7.50−7.53 (m, 1H, H3a), 7.21−7.24 (m, 1H, H5a), 7.24−7.18 (m, 2H, H6 and H3b), 6.87 (t, 1H, J = 7 Hz, H4), 6.82 (t, 1H, J = 7 Hz, H5), 6.74 (d, 1H, J = 7 Hz, H3), 4.13−4.06 (m, 4H, H7b and H7a), 3.36 (t, 2H, J = 6 Hz, H12), 3.22 (s, 3H, OCH_3), 2.79 (t, 2H, J = 8 Hz, H10), 2.40−2.36 (m, 2H, H11), 2.02−1.97 (m, 2H, H8), 1.34 (s, 6H, H7 and H7′). ^{1}H NMR (CD_2Cl_2, 600 MHz, −30 °C): δ 8.63 (d, 1H, J = 4 Hz, H6a), 8.43 (d, 1H, J = 4 Hz, H6b), 7.64−7.68 (m, 3H, H4a, H5b, and H4b), 7.52 (d, 1H, J = 7 Hz, H3a), 7.24−7.18 (m, 1H, H5a), 7.20−7.17 (m, 2H, H6 and H3b), 6.87 (t, 1H, J = 7 Hz, H4), 6.82 (t, 1H, J = 7 Hz, H5), 6.74 (d, 1H, J = 7 Hz, H3), 4.17−4.06 (m, 4H, H7a and H7b), 3.36 (t, 2H, J = 6 Hz, H12), 3.22 (s, 3H, OCH_3), 2.79 (t, 2H, J = 8 Hz, H10), 2.40−2.38 (m, 2H, H11), 2.01−1.97 (m, 2H, H8), 1.34 (s, 3H, H7), 1.33 (s, 3H, H7′). $^{13}C\{^1H\}$ NMR (CD_2Cl_2, 151 MHz, −30 °C): δ 168.31 (*CX1*), 159.56 (C2), 157.70 (C2b), 156.09 (C2a), 149.63 (C6a), 148.89 (C6b), 136.85 (C5b), 136.58 (C4b), 134.59 (C3b), 126.34 (C4a), 125.29 (C3a), 123.88 (C5), 123.28 (C5a), 122.98 (C6), 122.46 (C4), 121.57 (C3), 70.67 (C12), 63.03 (C7b), 62.77 (C7a), 58.34 (OCH_3), 55.44 (C10), 47.36 (C9), 43.84 (C8), 33.74 (C7), 33.17 (C7′), 27.70 (C11). MALDI MS (anthracene matrix): calcd for $[C_{26}H_{33}N_3OPd]^{\bullet+}$ m/z 509.9, obsd m/z 509.9.

General Procedure for the Synthesis of $[Pd^{IV}(CH_2CMe_2C_6H_4)(\kappa^3\text{-}N,N',N''\text{-}L1$ or $\text{-}L2)(X)]X$ Complexes (X = I, Br; 3−6). In air, to a solution of $[Pd^{II}(CH_2CMe_2C_6H_4)(\kappa^2\text{-}N,N'\text{-}\mathbf{L1})]$ (**1**; 0.019 g, 0.040 mmol) or $[Pd^{II}(CH_2CMe_2C_6H_4)(\kappa^2\text{-}N,N'\text{-}\mathbf{L2})]$ (**2**; 0.020 g, 0.040 mmol) in chloroform (2 mL) was added the appropriate oxidant (1 equiv) with vigorous stirring. After 5 min the solvent was evaporated, and the resulting powder was washed with ether (10 mL) and hexanes (5 mL) to remove residual impurities then dried under reduced pressure. All Pd^{IV} complexes were characterized and then stored as solids at −5 °C.

Synthesis of $[Pd^{IV}(CH_2CMe_2C_6H_4)(\kappa^3\text{-}N,N',N''\text{-}L1)I][I]$ (3). Upon addition of iodine (0.010 g, 0.040 mmol) a color change from light orange to dark red was observed. Yield: 78% (0.023 g, 0.031 mmol). ^{1}H NMR ($CDCl_3$, 600 MHz, 25 °C): δ 9.38 (d, 1H, J = 4 Hz, H6b), 9.11 (d, 1H, J = 4 Hz, H6a), 8.02 (d, 1H, J = 8 Hz, H3b), 7.88 (d, 1H, J = 8 Hz, H3a), 7.83 (t, 1H, J = 7 Hz, H4b), 7.73 (t, 1H, J = 7 Hz, H4a), 7.33 (t, 1H, J = 7 Hz, H5b), 7.29 (t, 1H, J = 7 Hz, H5a), 7.08 (t, 1H, J = 7 Hz, H5), 6.98 (dd, 1H, J = 7 Hz, 8 Hz, H6), 6.85 (t, J = 7 Hz, 1H, H4), 6.49 (d, 1H, J = 8 Hz, H3), 5.49 (d, 1H, J = 17 Hz, H7a), 5.35 (d, 1H, J = 16 Hz, H7b), 4.97 (d, 1H, J = 17 Hz, H7a′), 4.92 (d, 1H, J = 7 Hz, H8), 4.20 (d, 1H, J = 16 Hz, H7b′), 3.83−3.79 (m, 1H, H12), 3.74 (d, 1H J = 7 Hz, H8′), 3.59 (m, 1H, H10), 3.45−3.41 (m, 1H, H12), 2.70 (br, 1H, OH), 2.59−2.54 (m, 1H, H10), 2.38−2.34 (m, 1H, H11), 2.07−2.02 (m, 1H, H11), 1.53 (s, 3H, H7′), 1.48 (s, 3H, H7). $^{13}C\{^1H\}$ NMR ($CDCl_3$, 151 MHz, 25 °C): δ 160.19 (C2), 158.07 (C2a), 156.27 (C2b), 147.99 (C6b), 147.83 (C6a), 142.78 (C1), 139.86 (C4b), 139.66 (C4a), 131.57 (C3), 128.18 (C4), 126.98 (C5), 126.63 (C6), 125.60 (C3b), 125.30 (C5b), 124.97 (C5a), 124.45 (C3a), 65.35 (C7a), 65.11 (C7b), 61.91 (C8), 60.04 (C10), 59.72 (C12), 46.89 (C9), 32.20 (C7), 30.48 (C7′), 25.99 (C11). HRMS (ESI-TOF): calcd for $[C_{25}H_{31}IN_3OPd]^+$ m/z 622.0546, obsd m/z 622.0562. IR: ν(O−H) 3103 cm^{-1}. Orange crystals suitable for single-crystal X-ray crystallographic analysis were grown by the slow diffusion of pentane into an acetone solution of **3** at room temperature.

Synthesis of $[Pd^{IV}(CH_2CMe_2C_6H_4)(\kappa^3\text{-}N,N',N''\text{-}L2)I][I]$ (4). Upon addition of iodine (0.010 g, 0.040 mmol) a color change from light orange to dark brown was observed. Yield: 90% (0.026 g, 0.034 mmol). ^{1}H NMR ($CDCl_3$, 600 MHz, 25 °C): δ 9.31 (d, 1H, J = 5 Hz, H6b), 9.07 (d, 1H, J = 5 Hz, H6a), 8.08 (d, 1H, J = 8 Hz, H3b), 7.84 (d, 1H, J = 8 Hz, H3a), 7.76 (t, 1H, J = 8 Hz, H4b), 7.68 (t, 1H, J = 8 Hz, H4a), 7.27 (dd, 1H, J = 5 Hz, 8 Hz, H5b), 7.24−7.19 (m, 1H, H5a), 7.06 (t, 1H, J = 7 Hz, H5), 6.96 (d, 1H, J = 7 Hz, H6), 6.83 (t, 1H, J = 7 Hz, H4), 6.53 (d, 1H, J = 7 Hz, H3), 5.85 (d, 1H, J = 17 Hz, H7a′), 5.62 (d, 1H, J = 15 Hz, H7b′), 4.93 (d, 1H, J = 7 Hz, H8′), 4.53 (d, 1H, J = 17 Hz, H7a), 4.08 (d, 1H, J = 15 Hz, H7b), 3.62 (d, J = 7 Hz, 1H, H8), 3.43 (m, 1H, H12), 3.36−3.32 (m, 1H, H10), 3.17 (s, 3H, OCH_3), 3.18−3.13 (m, 1H, H12′), 2.43−2.39 (m, 1H, H11), 2.26−2.23 (m, 1H, H10′), 2.06−2.01 (m, 1H, H11′), 1.48 (s, 3H, H7′), 1.47 (s, 3H, H7). $^{13}C\{^1H\}$ NMR ($CDCl_3$, 151 MHz, 25 °C): δ 160.04 (C2), 157.79 (C2a), 156.32 (C2b), 147.72 (C6b), 147.60 (C6a), 143.07 (C1), 139.84 (C4b), 139.69 (C4a), 131.59 (C3), 128.18 (C4), 126.90 (C5), 126.51 (C6), 125.23 (C5b,C3b), 124.93 (C5a), 124.52 (C3a), 69.70 (C12), 65.09 (C7a), 64.82 (C7b), 61.23 (C10 and C8), 58.48 (OCH_3), 46.75 (C9), 32.23 (C7), 30.01 (C7′), 23.03 (C11). HRMS (ESI-TOF): calcd for $[C_{26}H_{33}IN_3OPd]^+$ m/z 636.0703, obsd m/z 636.0729. IR ν(methyl in O−CH_3) 2912 cm^{-1}.

Synthesis of $[Pd^{IV}(CH_2CMe_2C_6H_4)(\kappa^3\text{-}N,N',N''\text{-}L2)I][BF_4]$ (4a). Upon addition of bis(pyridine)iodonium(I) tetrafluoroborate (0.014 g, 0.040 mmol), in the dark, a color change from light orange to dark brown was observed. Yield: 80% (0.024 g, 0.033 mmol). ^{1}H NMR ($CDCl_3$, 600 MHz, 25 °C): δ 9.34 (d, 1H, J = 5 Hz, H6b), 9.09 (d, 1H, J = 5 Hz, H6a), 7.81−2.78 (m, 1H, H3b), 7.73 (d, 1H, J = 8 Hz, H3a), 7.60 (d, 1H, J = 8 Hz, H4b), 7.75−7.70 (m, 1H, H4a), 7.25−7.20 (m, 1H, H5b), 7.19−7.14 (m, 1H, H5a), 7.08 (d, 1H, J = 7 Hz, H5), 6.99 (d, J = 7 Hz, H6), 6.85 (t, 1H, J = 7 Hz, H4), 6.53 (d, 1H, J = 7 Hz, H3), 4.94 (d, 1H, J = 17 Hz, H7a), 4.77 (d, 1H, J = 15 Hz, H7b), 4.61 (d, 1H, J = 7 Hz, H8), 4.22 (d, 1H, J = 17 Hz, H7a), 3.65 (d, 1H, J = 15 Hz, H7b), 3.46 (d, J = 7 Hz, 1H, H8′), 3.42−3.39 (m, 1H, H12), 3.37−3.33 (m, 1H, H10), 3.18 (s, 3H, OCH_3), 3.17−3.14 (m, 1H, H12), 2.30−2.27 (m, 1H, H11), 2.26−2.22 (m, 1H, H10), 1.98−1.94 (m, 1H, H11), 1.50 (s, 3H, H7′), 1.49 (s, 3H, H7). ^{19}F NMR ($CDCl_3$, 564 MHz, 25 °C): δ −151.23. HRMS (ESI-TOF): calcd for $[C_{26}H_{33}IN_3OPd]^+$ m/z 636.0703, obsd m/z 636.0562.

Synthesis of $[Pd^{IV}(CH_2CMe_2C_6H_4)(\kappa^3\text{-}N,N',N''\text{-}L1)Br][Br]$ (5). Upon addition of bromine (2 μL, 0.04 mmol), an immediate color change from orange to light green was observed. Yield: 85% (0.022 g, 0.034 mmol). ^{1}H NMR ($CDCl_3$, 600 MHz, 25 °C): δ 9.04 (d, 1H, J = 4 Hz, H6b), 8.85 (d, 1H, J = 4 Hz, H6a), 7.94 (d, 1H, J = 8 Hz, H3b), 7.79−7.77 (m, 1H, H3a), 7.76−7.74 (m, 1H, H4b), 7.68 (t, 1H, J = 7 Hz, H4a), 7.30−7.28 (m, 1H, H5b), 7.21−7.19 (m, 1H, H5a), 7.07−7.04 (m, 1H, H5), 6.96 (d, 1H, J = 7 Hz, H6), 6.83 (t, 1H, J = 8 Hz, H4), 6.50 (d, 1H, J = 8 Hz, H3), 5.52 (d, 1H, J = 17 Hz, H7a), 5.47 (d, 1H, J = 16 Hz, H7b), 5.14 (d, 1H, J = 17 Hz, H7a′), 4.77 (d, 1H, J = 7 Hz, H8), (d, 1H, J = 16 Hz, H7b′), 4.03 (d, 1H, J = 7 Hz, H8′), 3.67−3.62 (m, 1H, H10), 3.70−3.66 (m, 1H, H12), 3.34−3.31 (m, 1H, H12′), 2.56−2.53 (m, 1H, H11), 2.39−2.36 (m, 1H, H10′), 2.07−2.03 (m, 1H, H11′), 1.51 (s, 3H, H7′), 1.48 (s, 3H, H7). $^{13}C\{^1H\}$ NMR ($CDCl_3$, 151 MHz, 25 °C): δ 158.79 (C1), 157.92 (C2b), 156.06 (C2a), 149.86 (C2), 146.73 (C6b), 146.46 (C6a), 139.95 (C4b), 139.81 (C4a), 129.48 (C3), 128.32 (C4), 126.93 (C6), 126.83 (C5), 125.02 (C5b), 124.95 (C3b), 124.55 (C5a), 124.03 (C3a), 67.73 (C8), 66.60 (C7a), 66.43 (C7b), 61.47 (C12), 59.51 (C10), 47.32 (C9), 33.10 (C7), 33.20 (C7′), 26.47 (C11). HRMS (ESI-TOF): calcd for $[C_{25}H_{31}BrN_3OPd]^+$ m/z 574.0685;

https://dx.doi.org/10.1021/acs.organomet.0c00615
Organometallics XXXX, XXX, XXX−XXX

obsd m/z 574.0706. IR: ν(O−H) 3361 cm^{-1}. Clear crystals suitable for single-crystal X-ray crystallographic analysis were grown by the slow diffusion of acetone into an acetonitrile solution of **5** at −15 °C.

*Synthesis of [Pd^{IV}(CH$_2$CMe$_2$C$_6$H$_4$)(κ^3-N,N′,N″-**L2**)Br][Br] (**6**).* Upon addition of bromine (2 μL, 0.04 mmol), an immediate color change from orange to green was observed. Yield: 80% (0.021 g, 0.031 mmol). ^{1}H NMR (CD$_2$Cl$_2$, 600 MHz, −8 °C): δ 9.04 (d, 1H, J = 4 Hz, H6b), 8.86 (d, 1H, J = 4 Hz, H6a), 7.91 (d, 1H, J = 8 Hz, H3b), 7.82−7.79 (m, 1H, H3a), 7.75−7.72 (m, 1H, H4b), 7.39−7.354 (m, 1H, H4a), 7.26−7.23 (m, 1H, H5b), 7.17−7.15 (m, 1H, H5a), 7.14−7.11 (m, 1H, H5), 7.03 (d, 1H, J = 8 Hz, H6), 6.90 (t, 1H, J = 8 Hz, H4), 6.62 (d, 1H, J = 8 Hz, H3), 5.93 (d, 1H, J = 17 Hz, H7a), 5.74 (d, 1H, J = 16 Hz, H7b), 4.65 (d, 1H, J = 17 Hz, H7a′), 4.80 (d, 1H, J = 6 Hz, H8), 4.25 (d, 1H, J = 16 Hz, H7b′), 3.88 (d, 1H, J = 6 Hz, H8′), 3.46−3.42 (m, 1H, H10), 3.40−3.37 (m, 1H, H12), 3.31−3.27 (m, 1H, H12), 3.17 (s, 3H, OCH$_3$), 2.33−2.37 (m, 2H, H11 and H10), 2.07−2.02 (m, 1H, H11), 1.51 (s, 3H, H7′), 1.50 (s, 3H, H7). ^{13}C{^{1}H} NMR (CD$_2$Cl$_2$, 600 MHz, −8 °C): δ 158.72 (C1), 157.30 (C2b), 155.91 (C2a), 150.19 (C2), 146.67 (C6b), 146.65 (C6a), 139.97 (C4b), 139.98 (C4a), 129.71 (C3), 128.57 (C4), 127.89 (C6), 126.83 (C5), 125.21 (C5b), 125.85 (C5a), 124.90 (C3b), 123.92 (C3a), 69.64 (C12), 66.89 (C8), 66.21 (C7a), 66.02 (C7b), 62.49 (C10), 58.48 (OCH$_3$), 47.12 (C9), 32.83 (C7), 28.86 (C7′), 23.42 (C11). HRMS (ESI-TOF): calcd for [C$_{26}$H$_{33}$BrN$_3$OPd]$^+$ m/z 588.0841, obsd, m/z 588.0468. IR: ν(methyl in O−CH$_3$) 2894 cm^{-1}.

Thermolysis Reactions from Pd(IV) Complexes. *General Procedure for the Analysis of Organic Products from Thermolysis.* To a solution of the Pd(IV) complex **3**−**6** (0.070 mmol) in CDCl$_3$ (2 mL), was added 1,3,5-trimethoxybenzene as an internal standard (0.023 mmol). A ^{1}H NMR spectrum was collected of the solution. The solution was stirred at 50 °C for 7.5 h (except for **4a**, which was stirred for 72 h). Then the solution was analyzed by ^{1}H and ^{1}H−^{1}H gCOSY NMR spectroscopy to identify and quantify the organics relative to the internal standard. In order to isolate the organics, the solutions were filtered through a plug of silica to remove the metal complexes, the silica was washed with CHCl$_3$ (3 × 5 mL), and the solvent was evaporated by rotary evaporation. The organic products were dissolved in chloroform for analysis by GC-MS.

*General Synthesis of [Pd^{II}(κ^3-N, N′,N″-**L1** or -**L2**)(X)]X Complexes (X = I, Br; **7**−**10**).* A solution of the Pd(IV) complex **3**−**6** (0.070 mmol) was dissolved in CHCl$_3$ (4 mL) and heated at 50 °C in an oil bath for 7.5 h. The solvent was removed under reduced pressure, and the residue was washed with ether (3 × 5 mL) and hexanes (3 × 5 mL) and then dried under vacuum. Thermolysis of complex **4a** was conducted by following the same procedure, except it was heated at 50 °C for 60 h.

*Synthesis of [Pd^{II}(κ^3-N,N′,N″-**L1**)I][I] (**7**).* A chloroform solution of **3** (0.042 g, 0.070 mmol) was dissolved in chloroform and heated to form **7**. Yield: 87% (0.036 g, 0.058 mmol). ^{1}H NMR (CDCl$_3$/CD$_3$OD, 600 MHz, 25 °C): δ 9.28 (d, 2H, J = 5 Hz, H6a), 7.96 (m, 2H, H4a), 7.74 (d, 2H, J = 7 Hz, H3a), 7.31 (t, 2H, J = 6 Hz, H5a), 5.24 (d, 2H, J = 16 Hz, H7a), 4.89 (d, 2H, J = 16 Hz, H7a′), 3.49−3.45 (m, 2H, H10), 3.21−3.16 (m, 2H, H12), 1.87−1.83 (m, 2H, H11). ^{13}C{^{1}H} NMR (CDCl$_3$/CD$_3$OD 1/0.3, 151 MHz, 25 °C): δ 164.74 (C2a), 156.47 (C6a), 140.77 (C4a), 125.61 (C3a), 123.85 (C5a), 67.89 (C7a, C7a′), 60.21 (C12), 58.55 (C10), 30.18 (C11). HRMS (ESI-TOF): calcd for [C$_{15}$H$_{19}$IN$_3$OPd]$^+$ m/z 489.960, obsd m/z 489.958. Anal. Calcd for C$_{15}$H$_{19}$I$_2$N$_3$OPd: C, 29.17; H, 3.10; N, 6.80. Found: C, 29.10; H, 3.05; N, 6.59. *Organic release step*: 1-Iodo-2-methyl-2-phenylpropane (**IP**): yield 37%. ^{1}H NMR (CDCl$_3$, 600 MHz, 25 °C): δ 7.27−7.33 (m, 5H, C$_6$H$_5$), 3.43 (s, 2H, CH$_2$), 1.50 (s, 6H, 2CH$_3$).[61] LR-MS: calcd for C$_{10}$H$_{13}$I m/z 260.12, obsd m/z 260.15. (2-Iodo-2-methylpropyl)benzene (**IB**): yield 28%. ^{1}H NMR (CDCl$_3$, 600 MHz, 25 °C): δ 7.21−7.35 (m, 5H, C$_6$H$_5$), 3.22 (s, 2H, CH$_2$), 1.96 (s, 6H, 2CH$_3$).[62] LR-MS: calcd for C$_{10}$H$_{13}$I m/z 260.12, obsd m/z 260.10. (2-Methylprop-1-en-1yl)benzene (**MB**): yield 20%. ^{1}H NMR (CDCl$_3$, 600 MHz, 25 °C): δ 7.27−7.35 (m, 2H, C$_6$H$_5$), 7.14−7.24 (m, 3H, C$_6$H$_5$), 6.27 (s, 1H, Ph-C*H*=CMe$_2$), 1.90 (s, 3H, CH$_3$), 1.86 (s, 3H, CH$_3$).[63] LR-MS: calcd for C$_{10}$H$_{12}$ m/z 132.21, obsd m/z 132.20. Dimethyl-1,2-dihydrocyclobutabenzene (**CB**): yield 5%. ^{1}H NMR (CDCl$_3$, 600 MHz, 25 °C): δ 8.01 (m, 1H, C$_6$H$_4$), 7.17 (m, 1H, C$_6$H$_4$), 7.07 (m, 1H, C$_6$H$_4$), 7.01 (m, 1H, C$_6$H$_4$), 2.99 (s, 2H, CH$_2$), 1.46 (s, 6H, Me).[19,28] LR-MS: calcd for C$_{10}$H$_{12}$ m/z 132.21, obsd m/z 132.20.

*Synthesis of [Pd^{II}(κ^3-N,N′,N″-**L2**)I][I] (**8**).* A chloroform solution of **4** (0.044 g, 0.070 mmol) was dissolved in chloroform and heated to form **8**. Yield: 91% (0.040 g, 0.061 mmol). ^{1}H NMR (CDCl$_3$, 600 MHz, 25 °C): δ 9.32 (d, 2H, J = 5 Hz, H6a), 7.98−7.95 (m, 2H, H5a), 7.90 (d, 2H, J = 8 Hz, H3a), 7.32 (t, 2H, J = 7 Hz, H4a), 5.62 (d, 2H, J = 16 Hz, H7a), 5.45 (d, 2H, J = 16 Hz, H7a′), 3.39−3.43 (m, 4H, H12 and H10), 3.23 (s, 3H, CH$_3$), 2.00−2.05 (m, 2H, H11). ^{13}C{^{1}H} NMR (CDCl$_3$, 151 MHz, 25 °C): δ 165.15 (C2a), 156.53 (C6a), 140.95 (C5a), 125.60 (C4a), 124.24 (C3a), 69.17 (C7a, C7a′), 69.08 (C12), 60.82 (C10), 58.77 (CH$_3$), 28.50 (C11). HRMS (ESI-TOF): calcd for [C$_{16}$H$_{21}$IN$_3$OPd]$^+$ m/z 503.9764, obsd m/z 503.9658. Anal. Calcd for C$_{16}$H$_{21}$I$_2$N$_3$OPd: C, 30.43; H, 3.35; N, 6.65. Found: C, 30.57; H, 3.73; N 6.48. Orange crystals suitable for single-crystal X-ray crystallographic analysis were grown by the slow diffusion of pentane into a dichloromethane solution of **8** at room temperature. *Organic release step*: **MB**, 48%; **IP**, 25%; **IB**, 8%; **CB**, 5%.

*Synthesis of [Pd^{II}(κ^3-N,N′,N″-**L2**)I][BF$_4$] (**8a**).* A chloroform solution of **4a** (0.050, 0.070 mmol) was dissolved in chloroform and heated for 60 h to form **8a**. Yield: 80% (0.034 g, 0.058 mmol). ^{1}H NMR (CDCl$_3$, 600 MHz, 25 °C): δ 9.30 (d, 2H, J = 5 Hz, H6a), 8.01−7.96 (m, 2H, H5a), 7.71 (d, 2H, J = 8 Hz, H3a), 7.34 (t, 2H, J = 8 Hz, H4a), 5.30 (d, 2H, J = 16 Hz, H7a), 4.66 (d, 2H, J = 16 Hz, H7a′), 3.34−3.39 (m, 2H, H12), 3.18 (s, 3H, CH$_3$), 3.13−3.15 (m, 2H, H10), 2.00−2.05 (m, 2H, H11). ^{13}C{^{1}H} NMR (CDCl$_3$, 151 MHz, 25 °C): δ 165.15 (C2a), 156.53 (C6a), 140.95 (C5a), 125.60 (C4a), 124.24 (C3a), 69.17 (C7a), 69.08 (C12), 60.82 (C10), 58.77 (CH$_3$), 28.50 (C11). HRMS (ESI-TOF): calcd for [C$_{16}$H$_{21}$IN$_3$OPd]$^+$ m/z 503.9764, obsd m/z 503.9658. *Organic release step*: **IP**, 13%; **MB**, 25%; **CB**, 30%.

*Synthesis of [Pd^{II}(κ^3-N,N′,N″-**L1**)Br][Br] (**9**).* A chloroform solution of **5** (0.040 g, 0.070 mmol) was dissolved in chloroform and heated to form **9**. Yield: 90% (0.031 g, 0.059 mmol). ^{1}H NMR ((CD$_3$)$_2$SO, 600 MHz, 25 °C): δ 8.86 (d, 2H, J = 5 Hz, H6a), 8.27−8.23 (m, 2H, H4a), 7.78 (d, 2H, J = 8 Hz, H3a), 7.67 (t, 2H, J = 7 Hz, H5a), 5.06 (d, 2H, J = 16 Hz, H7a), 4.56 (d, 2H, J = 16 Hz, H7a′), 3.39 (t, 2H, J = 6 Hz, H12), 3.13−3.10 (m, 2H, H10), 1.77−1.72 (m, 2H, H11). ^{13}C{^{1}H} NMR ((CD$_3$)$_2$SO, 151 MHz, 25 °C): δ 165.21 (C2a), 152.03 (C6a), 141.50 (C4a), 125.38 (C5a), 123.42 (C3a), 66.94 (C7a, C7a′), 60.55 (C10), 57.82 (C12), 30.83 (C11). HRMS (ESI-TOF): calcd for [C$_{15}$H$_{19}$BrN$_3$OPd]$^+$ m/z 441.9746, obsd m/z 441.9732. Yellow crystals suitable for single-crystal X-ray crystallographic analysis were grown by the slow diffusion of cyclohexane into a chloroform solution of **5** at room temperature. *Organic release step*: 1-bromo-2-methyl-2-phenylpropane (**BP**), 50%; **CB**, 28%; **MB**, 9%. ^{1}H NMR for **BP** (CDCl$_3$): δ(^{1}H) 7.27−7.33 (m, 5H, C$_6$H$_5$), 3.59 (s, 2H, CH$_2$), 1.48 (s, 6H, 2CH$_3$).[64] MS: calcd for C$_{10}$H$_{13}$Br m/z 213.12, obsd m/z 213.15.

*Synthesis of [Pd^{II}(κ^3-N,N′,N″-**L2**)Br][Br] (**10**).* A chloroform solution of **6** (0.040 g, 0.070 mmol) was heated to form **10**. Yield: 84% (0.038 g, 0.056 mmol). ^{1}H NMR ((CD$_3$)$_2$SO, 600 MHz, 25 °C): δ 8.80 (d, 2H, J = 5 Hz, H6a), 8.21−8.16 (m, 2H, H4a), 7.74 (d, 2H, J = 8 Hz, H3a), 7.62 (t, 2H, J = 7 Hz, H5a), 5.51 (d, 2H, J = 16 Hz, H7a), 4.50 (d, 2H, J = 16 Hz, H7a′), 3.11 (s, 3H, OCH$_3$), 2.67−2.70 (m, 2H, H12), 2.34−2.30 (m, 2H, H10), 1.49−1.45 (m, 2H, H11). LRMS (ESI-TOF): calcd for [C$_{16}$H$_{21}$BrN$_3$OPd]$^+$ m/z 455.99, obsd m/z 455.97. Anal. Calcd for C$_{16}$H$_{21}$Br$_2$N$_3$OPd: C, 35.75; H, 3.94; N, 7.82. Found: C, 35.81; H, 4.01; N, 7.59. Yellow crystals suitable for single-crystal X-ray crystallographic analysis were grown by the slow diffusion of cyclohexane into a dichloromethane solution of **6** at room temperature. *Organic release step*: **BP**, 24%; **CB**, 10%; **MB**, 50%.

*In Situ Synthesis of [Pd^{IV}(CH$_2$CMe$_2$C$_6$H$_4$)(κ^3-N,N′,N″-**L1**)Me][I] (**11**).* An NMR tube containing a CD$_2$Cl$_2$ solution (1.5 mL) of [Pd^{II}(CH$_2$CMe$_2$C$_6$H$_4$)(κ^2-N,N′-**L1**] (**1**; 0.028 g, 0.056 mmol) was inserted into the NMR instrument, and the probe was cooled to −30 °C. The NMR tube was ejected and precooled (−5 °C), CD$_3$I (10.5 μL, 0.169 mmol, 3 equiv) was added, and the tube was reinserted into

https://dx.doi.org/10.1021/acs.organomet.0c00615
Organometallics XXXX, XXX, XXX−XXX

the probe. The temperature was slowly increased to −10 °C. ^{1}H NMR (CD_2Cl_2, 600 MHz, −10 °C) 8.50 (d, 1H, J = 6 Hz, H6b), 8.32 (d, 1H, J = 6 Hz, H6a), 7.93 (t, 1H, J = 8 Hz, H4b), 7.81−7.75 (m, 1H, H4a), 7.70 (m, 2H, H3a and H3b), 7.48 (dd, 1H, J = 8 Hz, 6 Hz, H5b), 7.40 (dd, 1H, J = 8 Hz, 6 Hz, H5a), 7.01 (t, 1H, J = 7 Hz, H5), 6.84 (d, 1H, J = 7 Hz, H6), 6.74 (t, 1H, J = 7 Hz, H4), 6.08 (d, J = 7 Hz, 1H, H3), 4.82 (d, 1H, J = 17 Hz, H7a), 4.48 (d, 1H, J = 16 Hz, H7b), 4.19 (d, 1H, J = 17 Hz, H7a′), 4.13 (d, 1H, J = 16 Hz, H7b′), 3.64−3.60 (m, 1H, H12), 3.30 (m, 1H, H12), 3.27 (m, 1H, H8), 3.05 (d, 1H, J = 9 Hz, H8′), 2.74 (m, 1H, H10), 2.63 (m, 1H, H10), 1.81−1.76 (m, 1H, H11), 1.57−1.51 (m, 1H, H11′), 1.32 (s, 3H, H7), 1.27 (s, 3H, H7′). An analogous experiment was done, except with addition of CH_3I instead of CD_3I to characterize the Pd−CH_3 chemical shift. ^{1}H NMR (CD_2Cl_2, 600 MHz, −10 °C): 1.91 (s, 3H, Pd−CH_3). Reductive elimination to give **13** was observed at temperatures above 0 °C.

*In Situ Synthesis of [Pd^{IV}(CH$_2$CMe$_2$C$_6$H$_4$)(κ^3 -N,N′,N″-**L2**)Me][I] (**12**).* Complex **12** was made and characterized in a manner analogous to that for complex **11**. ^{1}H NMR (CD_2Cl_2, 600 MHz, −10 °C): δ 8.48 (d, 1H, J = 5 Hz, H6b), 8.34 (d, 1H, J = 5 Hz, H6a), 7.93 (t, 1H, J = 7 Hz, H4b), 7.80−7.75 (m, 1H, H4a), 7.65−7.71 (m, 2H, H3a and H3b), 7.48−7.42 (m, 1H, H5b), 7.41 (dd, 1H, J = 6 Hz, 8 Hz, H5a), 7.05 (t, 1H, J = 7 Hz, H5), 6.88 (d, 1H, J = 7 Hz, H6), 6.76−6.72 (m, 1H, H4), 6.21 (d, J = 8 Hz, 1H, H3), 4.78 (d, 1H, J = 16 Hz, H7a), 4.61 (d, 1H, J = 16 Hz, H7b), 4.49 (d, 1H, J = 16 Hz, H7a′), 4.40 (d, 1H, J = 16 Hz, H7b′), 3.50−3.54 (m, 1H, H12), 3.30−3.32 (m, 1H, H12′), 3.29−3.25 (m, 1H, H8), 3.14 (d, 1H, J = 9 Hz, H8′), 2.75−2.70 (m, 1H, *H10*), 2.66−2.62 (m, 1H, H10′), 1.85−1.80 (m, 1H, H11), 1.47−1.50 (m, 1H, H11′), 1.34 (s, 3H, H7), 1.31 (s, 3H, H7′). An analogous experiment was done, except with addition of CH_3I instead of CD_3I to characterize the Pd−CH_3 chemical shift. ^{1}H NMR (CD_2Cl_2, 600 MHz, −10 °C): δ 1.95 (s, 3H, Pd−CH_3). Reductive elimination from Pd(IV) was observed at temperatures above 0 °C.

*Synthesis of [Pd^{II}(CH$_2$CMe$_2$C$_6$H$_4$CH$_3$)(κ^3-N,N′,N″-**L1**)][I] (**13**).* To a solution of [Pd^{II}(CH$_2$CMe$_2$C$_6$H$_4$)(κ^2-N,N′-**L1**)] (**1**; 0.028 g, 0.056 mmol) in dichloromethane (2 mL) was added excess MeI (11 μL, 0.17 mmol, 3 equiv) with stirring. An immediate color change from orange to deep brown was observed. After the solvent was removed under reduced pressure, the orange product was washed with pentane (3 × 2 mL) and ether (3 × 2 mL) and dried under high vacuum. Yield: 78% (0.027 g, 0.043 mmol). ^{1}H NMR (CD_2Cl_2, 600 MHz, 25 °C): δ 8.26 (d, 2H, J = 5 Hz, H6a), 7.88 (t, 2H, J = 7 Hz, H4a), 7.61 (d, 2H, J = 7 Hz, H3a), 7.51 (d, 2H, J = 8 Hz, H3), 7.32 (t, 1H, J = 5 Hz, 7 Hz, H5a), 6.95−6.90 (m, 1H, H4), 6.77−6.72 (m, 2H, H6 and H5), 4.65 (d, 2H, J = 15 Hz, H7a), 4.50 (d, 2H, J = 15 Hz, H7a′), 3.37 (t, 2H, J = 5 Hz, H12), 2.82−2.78 (m, 2H, H10), 2.66 (s, 3H, CH_3), 2.23 (s, 2H, H8), 1.66−1.61 (m, 2H, H11), 1.57 (s, 6H, H7). ^{13}C{^{1}H} NMR (CD_2Cl_2, 151 MHz, 25 °C): δ 177.5 (C1), 163.93 (C2a), 149.29 (C6a), 148.20 (C2), 139.40 (C4a), 135.72 (C1), 132.64 (C5), 125.62 (C3), 125.60 (C6), 124.19 (C5a), 124.05 (C3a), 63.66 (C7a), 59.00 (C12), 54.53 (C10), 44.95 (C9), 43.56 (C8), 32.68 (C7), 29.4 (C11), 24.67 (CH_3). LRMS (ESI-TOF): calcd for [$C_{26}H_{34}N_3OPd$]$^+$ m/z 510.17, obsd m/z 510.19. IR: ν(O−H) 3337 cm^{-1}. For the sample used for the ^{2}H NMR experiment, CD_3I was used instead of CH_3I, while the rest of the reaction conditions were unchanged. ^{2}H NMR (CH_2Cl_2, 600 MHz, 25 °C): δ 2.66 (br, CD_3).

*Synthesis of [Pd^{II}(CH$_2$CMe$_2$C$_6$H$_4$−CH$_3$)(κ^3-N,N′,N″-**L2**)][I] (**14**).* Complex **14** was made in a manner analogous to that for complex **13**. Yield: 89% (0.032 g, 0.049 mmol). ^{1}H NMR (CD_2Cl_2, 600 MHz, 25 °C): δ 8.25 (d, 2H, J = 5 Hz, H6a), 7.89 (t, 2H, J = 7 Hz, H4a), 7.56 (d, 2H, J = 7 Hz, H3a), 7.53 (d, 1H, J = 8 Hz, H3), 7.32 (dd, 2H, J = 5 Hz, 7 Hz, H5a), 6.95−6.91 (m, 1H, H4), 6.76−6.72 (m, 2H, H6 and H5), 4.83 (d, 2H, J = 15 Hz, H7a), 4.48 (d, 2H, J = 15 Hz, H7a′), 3.17 (t, 2H, J = 6 Hz, H12), 3.10 (s, 3H, OCH_3), 2.76 (t, 2H, J = 8 Hz, H10), 2.66 (s, 3H, OCH_3), 2.25 (s, 2H, H8), 1.81 (br, 2H, H11), 1.57 (s, 6H, H7 and H7′). ^{13}C{^{1}H} NMR (CD_2Cl_2, 151 MHz, 25 °C): δ 164.06 (C1), 149.31 (C2a), 148.13 (C6a), 139.48 (C2), 135.73 (C4a), 132.68 (C1), 125.75 (C5 and C3), 124.24 (C6), 123.80 (C5a), 69.58 (C3a), 64.42 (C7a), 58.33 (C12), 55.48 (C10), 43.62 (C9), 40.75 (C8, C8′), 32.74 (C7, C7′), 27.50 (C11). ^{2}H experiment: ^{2}H NMR (CH_2Cl_2, 600 MHz, 25 °C) δ 3.10 (br, CD_3). LRMS (ESI-TOF): calcd for [$C_{27}H_{36}N_3OPd$]$^+$ m/z 524.19, obsd m/z 524.19. Anal. Calcd for $C_{27}H_{36}IN_3OPd$: C, 49.74; H, 5.56; N, 6.44. Found: C, 49.91; H, 5.28; N, 6.23. IR: ν(methyl in O−CH_3) 2868 cm^{-1}.

UV−Visible Studies. Complex **3** (0.017 g, 0.023 mmol) was dissolved in chloroform (2.8 mL) to give a 8.33 × 10^{-3} M solution. This solution was placed into a 4 mL cuvette (optical path length 1 cm) at room temperature and then heated to 50 °C. A UV−vis spectrum was recorded every 15 min for 7.5 h. The experiment was repeated twice to confirm the reproducibility. The observed rate constant, k_{obs}, was calculated by measuring the slope of the linear relationship between $\ln[A - A_\infty]/[A_0 - A_\infty]$ (A = absorbance) and time, for the first 2 h of heating (Table 2 and Figure 6). Data in the solvents methanol and benzene and for **4**−**6** were obtained in a similar way. For a study of the effect of free pyridine or sodium iodide on the rate, a solution in methanol of complex **3** (8.33 × 10^{-3} M) and pyridine or NaI (8.33 × 10^{-2} M) was prepared, and the rate of reductive elimination was determined as above (see Figures S62−S66).

X-ray Structure Determinations..[65−68] *Data Collection and Processing.* A crystal was mounted on a Mitegen polyimide micromount with a small amount of Paratone N oil. All X-ray measurements were made using a Bruker Kappa Axis Apex2 diffractometer at a temperature of 110 K. The frame integration was performed using SAINT, and the resulting raw data were scaled and the absorption was corrected using a multiscan averaging of symmetry-equivalent data using SADABS.

Structure Solution and Refinement. The structures were solved by using the SHELXT program. All non-hydrogen atoms were obtained from the initial solution. The hydrogen atoms were introduced at idealized positions and were allowed to ride on the parent atom. The structural model was fit to the data using full matrix least-squares based on F^2. The calculated structure factors included corrections for anomalous dispersion from the usual tabulation. The structure was refined using the SHELXL-2014 program from the SHELX suite of crystallographic software.[65−68] Details are given in Table S1.

■ ASSOCIATED CONTENT

Supporting Information

The Supporting Information is available free of charge at https://pubs.acs.org/doi/10.1021/acs.organomet.0c00615.

NMR, IR, and UV−vis spectra and crystallographic details (PDF)

Cartesian coordinates for the calculated structures (XYZ)

Accession Codes

CCDC 2031186−2031190 contain the supplementary crystallographic data for this paper. These data can be obtained free of charge via www.ccdc.cam.ac.uk/data_request/cif, or by emailing data_request@ccdc.cam.ac.uk, or by contacting The Cambridge Crystallographic Data Centre, 12 Union Road, Cambridge CB2 1EZ, UK; fax: +44 1223 336033.

■ AUTHOR INFORMATION

Corresponding Authors

Johanna M. Blacquiere − *Department of Chemistry, University of Western Ontario, London, Ontario, Canada N6A 5B7;* orcid.org/0000-0001-6371-6119; Email: johanna.blacquiere@uwo.ca

Richard J. Puddephatt − *Department of Chemistry, University of Western Ontario, London, Ontario, Canada N6A 5B7;* orcid.org/0000-0002-9846-3075; Email: pudd@uwo.ca

https://dx.doi.org/10.1021/acs.organomet.0c00615
Organometallics XXXX, XXX, XXX−XXX

Authors

Ava Behnia − *Department of Chemistry, University of Western Ontario, London, Ontario, Canada N6A 5B7*

Mahmood A. Fard − *Department of Chemistry, University of Western Ontario, London, Ontario, Canada N6A 5B7*

Complete contact information is available at: https://pubs.acs.org/10.1021/acs.organomet.0c00615

Author Contributions

All authors have given approval to the final version of the manuscript.

Funding

This work was financially supported by a Natural Sciences and Engineering Research Council (NSERC) of Canada Discovery Grant.

Notes

The authors declare no competing financial interest.

REFERENCES

(1) Sehnal, P.; Taylor, R. J. K.; Fairlamb, I. J. S. Emergence of Palladium(IV) Chemistry in Synthesis and Catalysis. *Chem. Rev.* **2010**, *110*, 824−889.

(2) Yin, G.; Mu, X.; Liu, G. Palladium(II)-Catalyzed Oxidative Difunctionalization of Alkenes: Bond Forming at a High-Valent Palladium Center. *Acc. Chem. Res.* **2016**, *49*, 2413−2423.

(3) Petrone, D. A.; Ye, J.; Lautens, M. Modern Transition-Metal-Catalyzed Carbon−Halogen Bond Formation. *Chem. Rev.* **2016**, *116*, 8003−8104.

(4) Giri, R.; Chen, X.; Yu, J.-Q. Palladium-Catalyzed Asymmetric Iodination of Unactivated C−H Bonds under Mild Conditions. *Angew. Chem., Int. Ed.* **2005**, *44*, 2112−2115.

(5) Zhou, M.-J.; Yang, T.-L.; Dang, L. Theoretical Studies on Palladium-Mediated Enantioselective C−H Iodination. *J. Org. Chem.* **2016**, *81*, 1006−1020.

(6) Zhang, B.; Yan, X.; Guo, S. Synthesis of Well-Defined High-Valent Palladium Complexes by Oxidation of Their Palladium(II) Precursors. *Chem. - Eur. J.* **2020**, *26*, 9430−9444.

(7) Canty, A. J. Development of organopalladium(IV) chemistry: fundamental aspects and systems for studies of mechanism in organometallic chemistry and catalysis. *Acc. Chem. Res.* **1992**, *25*, 83−90.

(8) Cámpora, J.; Palma, P.; Carmona, E. The chemistry of group 10 metalacycles. *Coord. Chem. Rev.* **1999**, *193*, 207−281.

(9) Canty, A. J.; van Koten, G. Mechanisms of d8 organometallic reactions involving electrophiles and intramolecular assistance by nucleophiles. *Acc. Chem. Res.* **1995**, *28*, 406−413.

(10) Canty, A. J. Organopalladium and platinum chemistry in oxidising milieu as models for organic synthesis involving the higher oxidation states of palladium. *Dalton Trans.* **2009**, 10409−10417.

(11) Xu, L.-M.; Li, B.-J.; Yang, Z.; Shi, Z.-J. Organopalladium(iv) chemistry. *Chem. Soc. Rev.* **2010**, *39*, 712−733.

(12) Racowski, J. M.; Sanford, M. S.; Canty, A. J. Carbon−Heteroatom Bond-Forming Reductive Elimination from Palladium-(IV) Complexes. *Top. Organomet. Chem.* **2011**, *35*, 61−84.

(13) Bonney, K. J.; Schoenebeck, F. Experiment and computation: a combined approach to study the reactivity of palladium complexes in oxidation states 0 to iv. *Chem. Soc. Rev.* **2014**, *43*, 6609−6638.

(14) Sberegaeva, A. V.; Watts, D.; Vedernikov, A. N.; Pérez, P. J. Oxidative Functionalization of Late Transition Metal−Carbon Bonds. *Adv. Organomet. Chem.* **2017**, *67*, 221−297.

(15) Yan, X.; Wang, H.; Guo, S. Employing Aryl-Linked Bis-mesoionic Carbenes as a Pincer-Type Platform to Access Ambient-Stable Palladium(IV) Complexes. *Angew. Chem., Int. Ed.* **2019**, *58*, 16907−16911.

(16) Nappi, M.; Gaunt, M. J. A Class of N−O-Type Oxidants To Access High-Valent Palladium Species. *Organometallics* **2019**, *38*, 143−148.

(17) Testa, C.; Roger, J.; Fleurat-Lessard, P.; Hierso, J.-C. Palladium-Catalyzed Electrophilic C−H-Bond Fluorination: Mechanistic Overview and Supporting Evidence. *Eur. J. Org. Chem.* **2019**, *2019*, 233−253.

(18) Puddephatt, R. J. Selectivity in carbon−carbon coupling reactions at palladium(IV) and platinum(IV). *Can. J. Chem.* **2019**, *97*, 529−537.

(19) Pérez-Temprano, M. H.; Racowski, J. M.; Kampf, J. W.; Sanford, M. S. Competition between sp3-C−N vs sp3-C−F Reductive Elimination from PdIV Complexes. *J. Am. Chem. Soc.* **2014**, *136*, 4097−4100.

(20) Pendleton, I. M.; Pérez-Temprano, M. H.; Sanford, M. S.; Zimmerman, P. M. Experimental and Computational Assessment of Reactivity and Mechanism in C(sp3)−N Bond-Forming Reductive Elimination from Palladium(IV). *J. Am. Chem. Soc.* **2016**, *138*, 6049−6060.

(21) Racowski, J. M.; Gary, J. B.; Sanford, M. S. Carbon(sp3)-Fluorine Bond-Forming Reductive Elimination from Palladium(IV) Complexes. *Angew. Chem., Int. Ed.* **2012**, *51*, 3414−3417.

(22) Canty, A. J.; Ariafard, A.; Camasso, N. M.; Higgs, A. T.; Yates, B. F.; Sanford, M. S. Computational study of C(sp3)-O bond formation at a PdIV centre. *Dalton Trans.* **2017**, *46*, 3742−3748.

(23) Camasso, N. M.; Canty, A. J.; Ariafard, A.; Sanford, M. S. Experimental and Computational Studies of High-Valent Nickel and Palladium Complexes. *Organometallics* **2017**, *36*, 4382−4393.

(24) Camasso, N. M.; Pérez-Temprano, M. H.; Sanford, M. S. C(sp3)−O Bond-Forming Reductive Elimination from PdIV with Diverse Oxygen Nucleophiles. *J. Am. Chem. Soc.* **2014**, *136*, 12771−12775.

(25) Qu, F.; Khusnutdinova, J. R.; Rath, N. P.; Mirica, L. M. Dioxygen activation by an organometallic Pd(ii) precursor: formation of a Pd(iv)-OH complex and its C-O bond formation reactivity. *Chem. Commun.* **2014**, *50*, 3036−3039.

(26) Cámpora, J.; López, J. A.; Palma, P.; Valerga, P.; Spillner, E.; Carmona, E. Cleavage of Palladium Metallacycles by Acids: A Probe for the Study of the Cyclometalation Reaction. *Angew. Chem., Int. Ed.* **1999**, *38*, 147−151.

(27) Nicasio-Collazo, J.; Wrobel, K.; Wrobel, K.; Serrano, O. Csp2−Br bond activation of Br-pyridine by neophylpalladacycle: formation of binuclear seven-membered palladacycle and bipyridine species. *New J. Chem.* **2017**, *41*, 8729−8733.

(28) Behnia, A.; Boyle, P. D.; Blacquiere, J. M.; Puddephatt, R. J. Selective Oxygen Atom Insertion into an Aryl−Palladium Bond. *Organometallics* **2016**, *35*, 2645−2654.

(29) Behnia, A.; Fard, M. A.; Blacquiere, J. M.; Puddephatt, R. J. Reactivity of a Palladacyclic Complex: A Monodentate Carbonate Complex and the Remarkable Selectivity and Mechanism of a Neophyl Rearrangement. *Organometallics* **2017**, *36*, 4759−4769.

(30) Sundaravel, K.; Sankaralingam, M.; Suresh, E.; Palaniandavar, M. Biomimetic iron(iii) complexes of N3O and N3O2 donor ligands: protonation of coordinated ethanolate donor enhances dioxygenase activity. *Dalton Trans.* **2011**, *40*, 8444−8458.

(31) Wu, J.-Z.; Bouwman, E.; Mills, A. M.; Spek, A. L.; Reedijk, J. Manganese(II) complexes of a set of 2-aminomethylpyridine-derived ligands bearing a methoxyalkyl arm: syntheses, structures and magnetism. *Inorg. Chim. Acta* **2004**, *357*, 2694−2702.

(32) Goldberg, J. M.; Berman, J. L.; Kaminsky, W.; Goldberg, K. I.; Heinekey, D. M. Oxidative addition of iodine to (tBu)4(POCOP)-Ir(CO) complexes. *J. Organomet. Chem.* **2017**, *845*, 171−176.

(33) Rogachev, A. Y.; Hoffmann, R. Iodine (I2) as a Janus-Faced Ligand in Organometallics. *J. Am. Chem. Soc.* **2013**, *135*, 3262−3275.

(34) Nabavizadeh, S. M.; Amini, H.; Rashidi, M.; Pellarin, K. R.; McCready, M. S.; Cooper, B. F. T.; Puddephatt, R. J. The mechanism of oxidative addition of iodine to a dimethylplatinum(II) complex. *J. Organomet. Chem.* **2012**, *713*, 60−67.

(35) Rendina, L. M.; Puddephatt, R. J. Oxidative Addition Reactions of Organoplatinum(II) Complexes with Nitrogen-Donor Ligands. *Chem. Rev.* **1997**, *97*, 1735−1754.
(36) Van Koten, G.; Van Beek, J. A. M.; Wehman-Ooyevaar, I. C. M.; Muller, F.; Stam, C. H.; Terheijden, J. Oxidative addition - reductive elimination reactions of mono- and bis(aryl)platinum(II) complexes with two amino ligands in fixed trans positions. X-ray crystal structures of (2,6-bis[[dimethylamino]methyl]phenyl)(4-tolyl)platinum(IV) diiodide and (2,6-bis[[dimethylamino]methyl]-phenyl)platinum(IV) trichloride. *Organometallics* **1990**, *9*, 903−912.
(37) Yang, L.; Powell, D. R.; Houser, R. P. Structural variation in copper(i) complexes with pyridylmethylamide ligands: structural analysis with a new four-coordinate geometry index, [small tau]4. *Dalton Trans.* **2007**, 955−964.
(38) Vigalok, A. Electrophilic Halogenation−Reductive Elimination Chemistry of Organopalladium and -Platinum Complexes. *Acc. Chem. Res.* **2015**, *48*, 238−247.
(39) Markies, B. A.; Canty, A. J.; Boersma, J.; van Koten, G. Phenylpalladium(IV) Chemistry: Selectivity in Reductive Elimination from Palladium(IV) Complexes and Alkyl Halide Transfer from Palladium(IV) to Palladium(II). *Organometallics* **1994**, *13*, 2053−2058.
(40) Jawad, J. K.; Puddephatt, R. J.; Stalteri, M. A. Selectivity in reactions of alkyl-aryl-transition-metal complexes with electrophiles. *Inorg. Chem.* **1982**, *21*, 332−337.
(41) Shaw, P. A.; Rourke, J. P. Selective C-C coupling at a Pt(iv) centre: 100% preference for sp2-sp3 over sp3-sp3. *Dalton Trans.* **2017**, *46*, 4768−4776.
(42) Bowes, E. G.; Pal, S.; Love, J. A. Exclusive Csp3−Csp3 vs Csp2−Csp3 Reductive Elimination from PtIV Governed by Ligand Constraints. *J. Am. Chem. Soc.* **2015**, *137*, 16004−16007.
(43) Anderson, C. M.; Crespo, M.; Kfoury, N.; Weinstein, M. A.; Tanski, J. M. Regioselective C−H Activation Preceded by Csp2−Csp3 Reductive Elimination from Cyclometalated Platinum(IV) Complexes. *Organometallics* **2013**, *32*, 4199−4207.
(44) Shaw, P. A.; Clarkson, G. J.; Rourke, J. P. Long-Lived Five-Coordinate Platinum(IV) Intermediates: Regiospecific C−C Coupling. *Organometallics* **2016**, *35*, 3751−3762.
(45) Goldberg, K. I.; Yan, J.; Breitung, E. M. Energetics and Mechanisms of Carbon-Carbon and Carbon-Iodide Reductive Elimination from a Pt(IV) Center. *J. Am. Chem. Soc.* **1995**, *117*, 6889−6896.
(46) Brown, M. P.; Puddephatt, R. J.; Upton, C. E. E. Mechanism of reductive elimination of ethane from some halogenotrimethylbis-(tertiary phosphine)platinum(IV) complexes. *J. Chem. Soc., Dalton Trans.* **1974**, 2457−2465.
(47) Grice, K. A.; Scheuermann, M. L.; Goldberg, K. I.; Canty, A. J. Five-Coordinate Platinum(IV) Complexes. *Top. Organomet. Chem.* **2011**, *35*, 1−27.
(48) Puddephatt, R. J. Coordinative Unsaturation in Platinum(IV) Chemistry: From Proposed Reaction Intermediates to the First Structurally Characterized Complexes. *Angew. Chem., Int. Ed.* **2002**, *41*, 261−263.
(49) Byers, P. K.; Canty, A. J.; Crespo, M.; Puddephatt, R. J.; Scott, J. D. Reactivity and mechanism in oxidative addition to palladium(II) and reductive elimination from palladium(IV) and an estimate of the palladium methyl bond energy. *Organometallics* **1988**, *7*, 1363−1367.
(50) Behnia, A.; Fard, M. A.; Blacquiere, J. M.; Puddephatt, R. J. Mild and selective Pd−Ar protonolysis and C−H activation promoted by a ligand aryloxide group. *Dalton Trans.* **2018**, *47*, 3538−3548.
(51) Shubin, V. G., Rearrangements of carbocations by 1,2-shifts. In *Contemporary Problems in Carbonium Ion Chemistry I/II*; Rees, C., Ed.; Springer Berlin Heidelberg: Berlin, Heidelberg, 1984; pp 267−341.
(52) Cámpora, J.; Palma, P.; del Río, D.; Carmona, E.; Graiff, C.; Tiripicchio, A. Nitrosyl, Nitro, and Nitrato Complexes of Palladium-(IV). The First Structurally Characterized Mononuclear Nitrosyl Complex of Palladium. *Organometallics* **2003**, *22*, 3345−3347.
(53) Heck, R.; Winstein, S. Neighboring Carbon and Hydrogen. XXIX. ρ-σ Analysis of Acetolysis of Substituted Neophyl Arylsulfonates. *J. Am. Chem. Soc.* **1957**, *79*, 3432−3438.
(54) Saunders, W. H.; Paine, R. H. Phenyl vs. Methyl Migration Aptitudes in Some Carbonium Ion Reactions of Neophyl Derivatives1. *J. Am. Chem. Soc.* **1961**, *83*, 882−885.
(55) Cámpora, J.; Gutiérrez-Puebla, E.; López, J. A.; Monge, A.; Palma, P.; del Río, D.; Carmona, E. Cleavage of the Calkyl−Caryl Bond of [Pd−CH2CMe2Ph] Complexes. *Angew. Chem., Int. Ed.* **2001**, *40*, 3641−3644.
(56) In methanol, complex **4** gave about equal amounts of **XP** and **XB** with X = I or OMe, the latter involving solvolysis by methanol.
(57) te Velde, G.; Bickelhaupt, F. M.; Baerends, E. J.; Fonseca Guerra, C.; van Gisbergen, S. J. A.; Snijders, J. G.; Ziegler, T. Chemistry with ADF. *J. Comput. Chem.* **2001**, *22*, 931−967.
(58) Becke, A. D. Density-functional exchange-energy approximation with correct asymptotic behavior. *Phys. Rev. A: At., Mol., Opt. Phys.* **1988**, *38*, 3098−3100.
(59) Drew, D.; Doyle, J. R.; Shaver, A. G. Cyclic Diolefin Complexes of Platinum and Palladium. *Inorg. Synth.* **2007**, 47−55.
(60) Bailey, C. T.; Lisensky, G. C. Synthesis of organometallic palladium complexes: An undergraduate experiment. *J. Chem. Educ.* **1985**, *62*, 896.
(61) Collman, J. P.; Brauman, J. I.; Madonik, A. M. Oxidative Addition Mechanisms of a Four-Coordinate Rhodium (I) Macrocycle. *Organometallics* **1986**, *5*, 310−322.
(62) Kiyokawa, K.; Watanabe, T.; Fra, L.; Kojima, T.; Minakata, S. Hypervalent Iodine(III)-Mediated Decarboxylative Ritter-Type Amination Leading to the Production of α-Tertiary Amine Derivatives. *J. Org. Chem.* **2017**, *82*, 11711−11720.
(63) Frlan, R.; Sova, M.; Gobec, S.; Stavber, G.; Časar, Z. Cobalt-Catalyzed Cross-Coupling of Grignards with Allylic and Vinylic Bromides: Use of Sarcosine as a Natural Ligand. *J. Org. Chem.* **2015**, *80*, 7803−7809.
(64) Tamao, K.; Yoshida, J.-i.; Akita, M.; Sugihara, Y.; Iwahara, T.; Kumada, M. Organofluorosilicates in Organic Synthesis. XVI. Synthesis of Organopentafluorosilicates via the Diels-Alder, Ene, and Friedel-Crafts Reaction. Their Transformations to Organic Halides and Alcohols. *Bull. Chem. Soc. Jpn.* **1982**, *55*, 255−260.
(65) *SAINT, ver. 2013.8*; Bruker-Nonius: Madison, WI 53711, USA, 2013.
(66) *SADABS, ver. 2012.1*; Bruker-Nonius: Madison, WI 53711, USA, 2012.
(67) Sheldrick, G. SHELXT - Integrated space-group and crystal-structure determination. *Acta Crystallogr., Sect. A: Found. Adv.* **2015**, *A71*, 3−8.
(68) Sheldrick, G. Crystal structure refinement with SHELXL. *Acta Crystallogr., Sect. C: Struct. Chem.* **2015**, *71*, 3−8.

https://dx.doi.org/10.1021/acs.organomet.0c00615
Organometallics XXXX, XXX, XXX−XXX